

Design of “Sensor Bot” for Evaluating Sensor Suites

Final Report

Submitted to:

Ninaad Damis, Software Developer II
Tailor
Austin, Texas



Prepared by:

Talal Al-Otaibi, Team Leader
Phillip Gavino
Rahul Kalakuntla
Jack Qiao

Mechanical Engineering Design Projects Program
The University of Texas at Austin
Austin, Texas

Fall 2023

ACKNOWLEDGEMENTS

The Tailos team would like to thank all the people and organizations that supported this project. Firstly, the team would like to thank Tailos Inc. and Ninaad Damis for being excellent sponsors during the semester. The constant contact and open advice throughout this project's time span allowed the team to flourish and achieve many of the deliverables tasked to the group.

The team would also like to thank Dr. David Fridovich-Keil for his useful advice at the beginning of this project. The team members who worked on the software for this project came into it with novice knowledge about how to use the robot operating system (ROS). Dr. Fridovich-Keil gave great pointers on how to use this technology, which helped tremendously.

Finally, the team would like to thank Dr. Richard Crawford and the ME266K TA's and staff for their guidance and facilitation of this project. The knowledge that came from the course lectures and advice from the team's TA, Gehan Jayatilaka, aided with the understanding and execution of the proper methodologies, analyses, and most importantly, the justifications for how and why the team made certain engineering decisions.

TABLE OF CONTENTS

| | |
|---|-----|
| Acknowledgements | i |
| Table of Contents | iii |
| List of Figures | vii |
| List of Tables | ix |
| Executive Summary | ix |
| 1 BACKGROUND | 1 |
| 1.1 Sponsor and Faculty Advisor | 1 |
| 1.2 Senior Design Team | 2 |
| 1.3 Patents Search | 3 |
| 1.3.1 Inside of a Vacuum Cleaning Robot | 4 |
| 1.3.2 Optical Table Mounting Platform\..... | 5 |
| 1.3.3 Electronic Device Ball and Socket Joint Mount | 6 |
| 1.4 Hardware Research | 7 |
| 1.4.1 NVIDIA Jetson | 7 |
| 2 PROBLEM STATEMENT | 8 |
| 2.1 Problem Background | 8 |
| 2.2 Problem Statement | 9 |
| 3 REQUIREMENTS AND CONSTRAINTS | 10 |
| 3.1 Requirements | 13 |
| 3.2 Constraints | 14 |
| 4 DELIVERABLES | 16 |
| 4.1 Specific Deliverables | 16 |
| 4.2 Cost Estimation | 16 |
| 5 MECHANICAL DESIGN | 17 |
| 5.1 Mechanical Idea Generation | 17 |
| 5.2 Mechanical Idea Selection | 26 |
| 5.3 Final Mechanical Design | 28 |
| 6 SOFTWARE DESIGN | 35 |
| 6.1 Software Decisions | 36 |
| 6.2 Electrical Hardware & Software Execution | 37 |
| 7 RESULTS & ANALYSIS | 40 |
| 7.1 Physical Prototype | 40 |
| 7.2 Collision Analysis | 41 |
| 7.3 Vibrational Analysis | 42 |
| 8 ECONOMIC ANALYSIS | 47 |
| 9 CONCLUSION & RECOMMENDATIONS | 49 |
| References | 51 |
| APPENDIX A: DATA SHEETS | A-1 |
| APPENDIX B: MORPHOLOGICAL MATRICES | B-1 |
| APPENDIX C: BACK OF ENVELOPE CALCULATIONS (BOE) | C-1 |
| APPENDIX D: PUGH CHARTS | D-1 |
| APPENDIX E: BILL OF MATERIALS | E-1 |
| APPENDIX F: GANTT CHART | F-1 |

LIST OF FIGURES

| | | |
|-------------|---|-----|
| Figure 1. | Rosie robot model (Tailos, 2023). | 1 |
| Figure 2. | Diagram of the inside of a vacuum cleaning robot (Lee, 2017). | 5 |
| Figure 3. | Image of an optical breadboard for component mounting (Farmiga, 1998). | 6 |
| Figure 4. | Sketch of an electronic device ball and socket joint mount (Kalis, 2007). | 7 |
| Figure 5. | Image of the Jetson Orin Nano (NVIDIA, 2020). | 8 |
| Figure 6. | Minimum and ideal coverage (Tailos, 2023). | 11 |
| Figure 7. | Blackbox diagram of the sensor mount system. | 18 |
| Figure 8. | Functional tree of the sensor mount. | 19 |
| Figure 9. | Image of the sensor mount mind-map. | 21 |
| Figure 10. | Sketch of the Optical Table design. | 23 |
| Figure 11. | Sketch of the Magnet design. | 24 |
| Figure 12. | Carbon fiber tube side view. | 25 |
| Figure 13. | Aluminum extrusion design. | 26 |
| Figure 14. | An image of the Jetson enclosure. | 29 |
| Figure 15. | An image of the perimeter mounting solution. | 30 |
| Figure 16. | An image of the V2 degree-ratcheting mount. | 31 |
| Figure 17. | Image of a sensor mount combination. | 32 |
| Figure 18. | Rendered view of optical table design. | 33 |
| Figure 19. | Image of the quarter panel integration. | 34 |
| Figure 20. | Rendering of Sensor Suite Platform assembly w/ mock sensor suite. | 35 |
| Figure 21. | Rosie spinning with Jetson teleoperation. | 38 |
| Figure 22. | Black box diagram of the sensor evaluation suite. | 38 |
| Figure 23. | Black box diagram of the sensor evaluation suite. | 39 |
| Figure 24. | PID controller for odometry and robot position control. | 39 |
| Figure 25. | Image of the physical prototype. | 41 |
| Figure 26. | Image of the 23 rd step of a universal mount collision FEA stress result. | 42 |
| Figure 27. | Vibrational measurement setup. | 43 |
| Figure 28. | Sensor mount linear acceleration raw measurements (left). Acceleration requeency response (right). | 44 |
| Figure 29. | Displacement numerical integration results. | 44 |
| Figure 30. | Short-term Fourier transform analysis to analyze time-dependent frequencies. | 45 |
| Figure A.1. | Image of the Jeston Orin Nano data sheet (NVIDIA, 2022). | A-1 |
| Figure A.2. | Image of the carbon fiber tube data sheet (McMaster, 2023). | A-3 |
| Figure A.3. | Image of the magnet strip data sheet (McMaster, 2023). | A-4 |
| Figure A.4. | Image of the aluminum extrusion data sheet (80/20, 2023). | A-5 |
| Figure C.1. | BOE calculations for mass and cost of the optical table design. | C-1 |
| Figure C.2. | BOE calculations for degrees of freedom (DOF) and mounting positions of the rectangular platform. | C-2 |
| Figure C.3. | BOE calculations for mass and cost of the aluminum extrusion design. | C-3 |
| Figure C.4. | BOE calculations for DOF and mounting positions of the rectangular beams. | C-4 |
| Figure C.5. | BOE calculations for mass and cost of the carbon fiber tube design. | C-5 |

| | | |
|-------------|---|-----|
| Figure C.6. | BOE calculations for DOF and mounting positions of the cylindrical beams. | C-6 |
| Figure C.7. | BOE calculations for mass and cost of the magnets design. | C-7 |
| Figure C.8. | BOE calculations for DOF and mounting positions of the ball & socket. | C-8 |
| Figure F.1. | Image of the Gantt chart. | F-3 |

LIST OF TABLES

| | | |
|------------|---|-----|
| Table 1. | The Tailos team’s specifications sheet. | 12 |
| Table 2. | Morphological matrix table..... | 22 |
| Table A.1. | The different sensors and use cases (Tailos, 2023)..... | A-2 |
| Table B.1. | Optical table with rectangular outer frame. | B-1 |
| Table B.2. | Aluminum extrusion with rectangular outer frame design. | B-1 |
| Table B.3. | Magnets with arm & socket joints design..... | B-2 |
| Table B.4. | Carbon fiber tubes with cylindrical outer frame design..... | B-2 |
| Table D.1. | Pugh chart with the Optical Table design as the datum..... | D-1 |
| Table D.2. | Pugh chart with the Aluminum Extrusion design as the datum..... | D-1 |
| Table D.3. | Pugh chart with the Carbon Fiber Tubes design as the datum..... | D-2 |
| Table D.4. | Pugh chart with the Magnets design as the datum..... | D-2 |
| Table E.1. | Bill of Materials table. | E-1 |

EXECUTIVE SUMMARY

The project, sponsored by Tailos, an Austin-based startup specializing in intelligent robot vacuums for hospitality, aimed to enhance the capabilities of their leading PD1 robot platform, known as Rosie. The senior design team collaborated with Ninaad Damis, point of contact from Tailos.

The central problem statement in question was developing a universal sensor mounting platform for Rosie to facilitate testing various sensor configurations. This problem statement arose from the motivation to optimize their robot's sensor suite to hotel cleaning environments and expand its capabilities to carry out stair and human detection.

The project was guided by a set of precise functional requirements and constraints, focusing on the field of view (FOV), sensor placement flexibility, and vibrational stability. These requirements were formulated based on direct inputs from Tailos and an analysis of their current product specifications. The design had to accommodate different sensor suites while ensuring stability, accuracy, and adaptability under operational conditions.

The deliverables included a modular sensor mounting platform, supporting the ability to reposition all four provided sensors. Presented as both a CAD model and a physical construction, the platform was designed to cater to a wide range of sensor FOVs. Integration of the Nvidia Jetson Orin Nano with the robot's existing systems was also a key hardware and software deliverable. Moreover, a ROS-based software architecture sought to leverage RViz to provide a sensor coverage visualization platform based on the combined positioning of all sensors.

The mechanical design process involved idea generation, selection, and final design, using methods like functional modeling, morphological matrices, and Pugh charts. The team focused on creating a design that would mount and position the sensors as well as secure the electronics. Various concepts, such as using an optical table design, a magnet grid, and a carbon fiber tube or aluminum extrusion frame, were explored. The final design evolved to accommodate the need to conform to the robot's aesthetics, resulting in a design consisting of fully 3D printed ratchet mounts, railed perimeter mounts, and an optical breadboard.

The software design revolved around replacing the robot's current IMX8 microcontroller with a Nvidia Jetson, ensuring compatibility with Tailos's existing codebase. The team adopted a workflow involving ROS2, Docker containerization, and remote protocols, facilitating robust development and integration of actuators and sensors.

The project culminated in a fully teleoperational physical prototype, which underwent rigorous testing through simulations and experiments, including collision and vibrational analyses. These analyses validated the robustness and stability of the universal mount assembly, ensuring that it could withstand real-world operational dynamics. Future work recommendations consist of actuating the sensor mounts and using the final CAD design and parameterizing sensor positions as inputs to RViz for simulated sensor coverage.

1 BACKGROUND

1.1 Sponsor and Faculty Advisor

The sponsor for the senior design team's project is Tailos, an automation-based startup out of Austin, Texas that builds intelligent robot vacuums for labor intensive industries, with most current applications in the field of hospitality. Below is a model of Tailos' most commercially available robot, Rosie. The robot utilizes a robust AI path planning platform to navigate spaces and efficiently clean the floor.

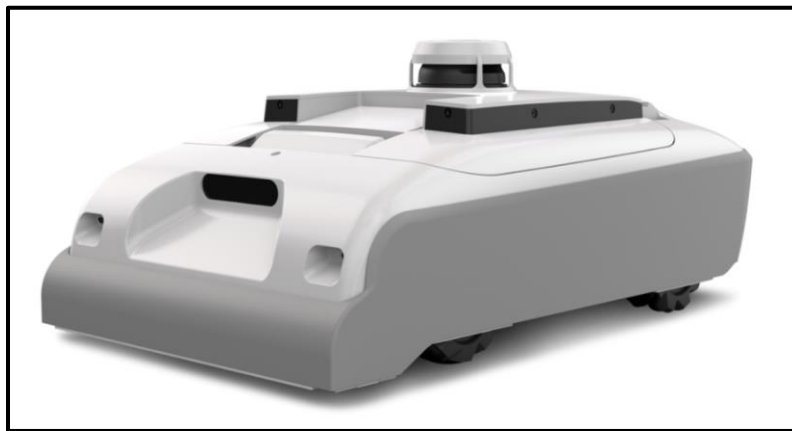


Figure 1. Rosie robot model (Tailos, 2023).

The Tailos team's faculty advisor for this project is Dr. David Fridovich-Keil. He is an assistant professor working in the Aerospace Engineering and Engineering Mechanics department at the University of Texas at Austin (UT Austin). His department research is in controls, autonomy, and robotics with a relevant research interest in motion planning. The senior design team aims to meet with Dr. Fridovich-Keil frequently to gain insight into sensor positioning and evaluation.

1.2 Senior Design Team

The senior design team is composed of 4 mechanical engineering students in-residence at UT Austin. This team's interests include computation-driven mechanical design, robots and mechatronics, high-level software design and low-level embedded system programming.

Talal Al-Otaibi is an undergraduate mechanical engineering student specializing in mechatronics, robotics, and computational engineering. His work experience encompasses the rapprochement of embedded systems and signal processing with dynamic systems and controls. Talal's past projects include the development of an atomic force microscope with a heavy emphasis on loop shaping control techniques and error budgeting. He also worked on a low-cost augmented reality prototype to carry out a simulated weld via a one-camera system using openCV. Currently, he is conducting IMU based sensor fusion research and development for unmanned underwater vehicles at UT's Applied Research Labs. All these experiences have provided a solid background for multidisciplinary work to be done on this project.

Phillip Gavino is an integrated undergraduate/graduate mechanical engineering student at UT Austin. He has a certificate in computer science and focuses on manufacturing and design. Phillip worked as an undergraduate research assistant for multiple professors in both the robotics and complex systems fields. Two experiences that are relevant to this project are when he worked with haptics for surgical applications and soft robotics for manufacturing. These experiences justify Phillip's aptitude in mechatronic and robotic design, demonstrating the value he brings to this project.

Rahul Kalakuntla is an undergraduate mechanical engineering student at UT Austin specializing in mechanical/computational/parametric design, DFM/DFAM, and autonomous systems. His recent work deals with scalable mechanical design and design optimization. Currently he is working on a series of personal projects that include conformal lattice design optimization, topology optimization, and end-use additive manufacturing techniques.

Jack Qiao is an integrated undergraduate/graduate mechanical engineering student at UT Austin. He has experience in control engineering, image processing, machine learning, computer vision, and mechatronics. He is currently working with NASA Glenn Research Center in developing advanced microscopy methods under microgravity and designing electromagnetic suspension systems for Texas Guadalupe. After graduation, Jack hopes to work in engineering consulting or private sector R&D.

1.3 Patents Search

To start the Tailos team's design research, they searched online for different patents and their sketches/diagrams for good idea references. Things they focused on were complete robot vacuum diagrams and mounting apparatuses.

Given that the nature of this project, further outlined in the upcoming sections, revolves around the creation of a testing tool for the development of future system iterations as opposed to engineering a market solution/product directly, this patent search is not solely justified by the need to avoid infringement of intellectual property; Rather, there are more specific purposes. Tailos is heavily motivated by shaping its robots to operate in closed environments for the purpose of housekeeping; this motivates the need to improve the intelligence and algorithmic capabilities of its current robots to be more well

suited for this function. To do so, the selection and configuration of these sensors need to be well tuned. By carrying out a patent search, prior art is researched and helps define an understanding of developments that have taken place in this emerging industry. Therefore, design solutions can be informed by the presence of these existing products as a starting point for idea generation. Moreover, a patents search provides insights to what possible past and current robotics experts are working on. This provides a sense of direction for any research & development goals needed to develop improved iterations that exceed current standards of performance for an autonomous system. Finally, a patent search helps constrain the range of possible equipment and hardware needed for the fulfillment of this engineering project, tying back to the point of idea generation moving forward.

1.3.1 Inside of a Vacuum Cleaning Robot

Patent 10,918,250 provides information on an improved robot vacuum cleaner with increased cleaning performance with reduced suction power in walled areas (Lee, 2017). This robot comprises a main body that is driven on a floor and sucks in debris via an impeller. This design is of interest due to the position of the controller it uses. This controller sits in the back of the robot, a design choice that allows the main drive train and suction subsystems to perform well without an awkward controller getting in the way. Figure 2 shows a diagram of the robot. The enclosure on the back of the inner body is where the controller is located.

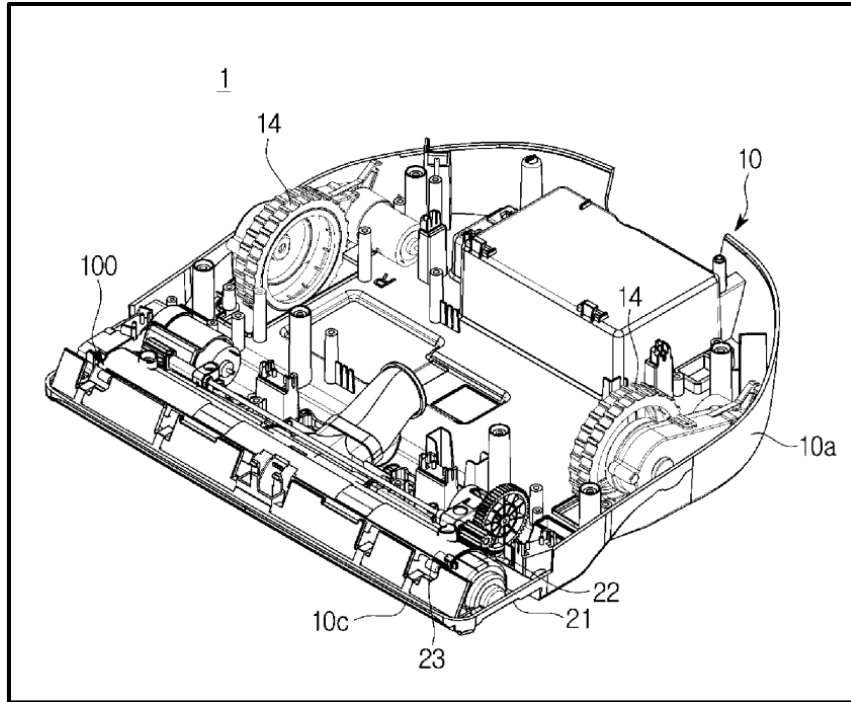


Figure 2. Diagram of the inside of a vacuum cleaning robot (Lee, 2017).

1.3.2 Optical Table Mounting Platform\

The optical table is designed to universally accept custom sensor mounts. Figure 3, from patent number 7,296,771, below shows an example of three sensors which mount to a generic optical breadboard. These sensor mounts are not ideal but establish a good starting point on how to design around an optical breadboard with multibody components connected simply with fasteners. Also, these designs allow for multiple kinds of sensors to be mounted onto the main mounting faces, a good idea for how to reduce the number of individual mounts. As a major requirement is production-level repeatability, a universal sensor mount is necessary: one that homogenizes all orientations of mounting holes for the team's given sensor stack and mounts in a repeatable way to the optical table.

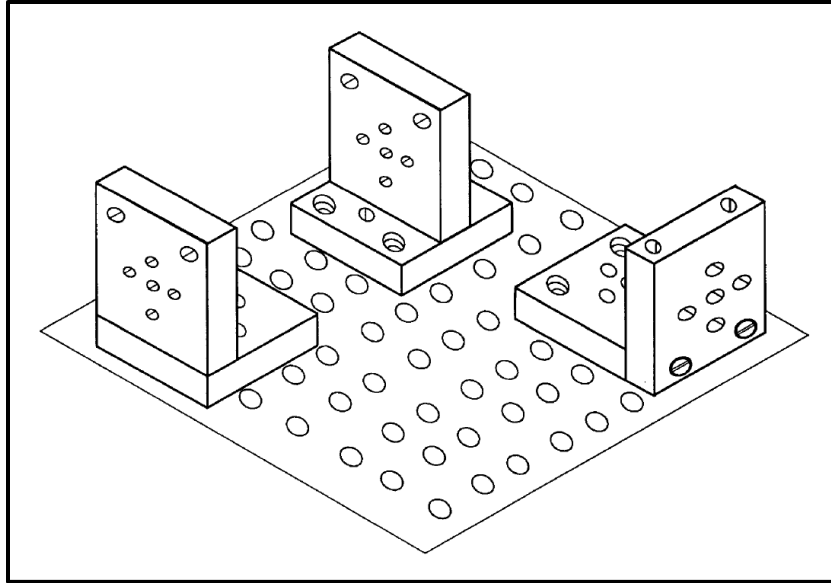


Figure 3. Image of an optical breadboard for component mounting (Farmiga, 1998).

1.3.3 Electronic Device Ball and Socket Joint Mount

From patent 5,825,558, Figure 4 shows a sketch of a three degree of freedom universal mounting system for electronic devices. This was searched for do to the objective of this project being mounting different cameras and sensors onto a mounting platform. This design consists of two main parts, the mounting face with ball on the end and the socket piece that mounts to any kind of flat surface. This is ideal for a flat platform that lacks any rotational positioning and adds more functionality to a simple plate design.

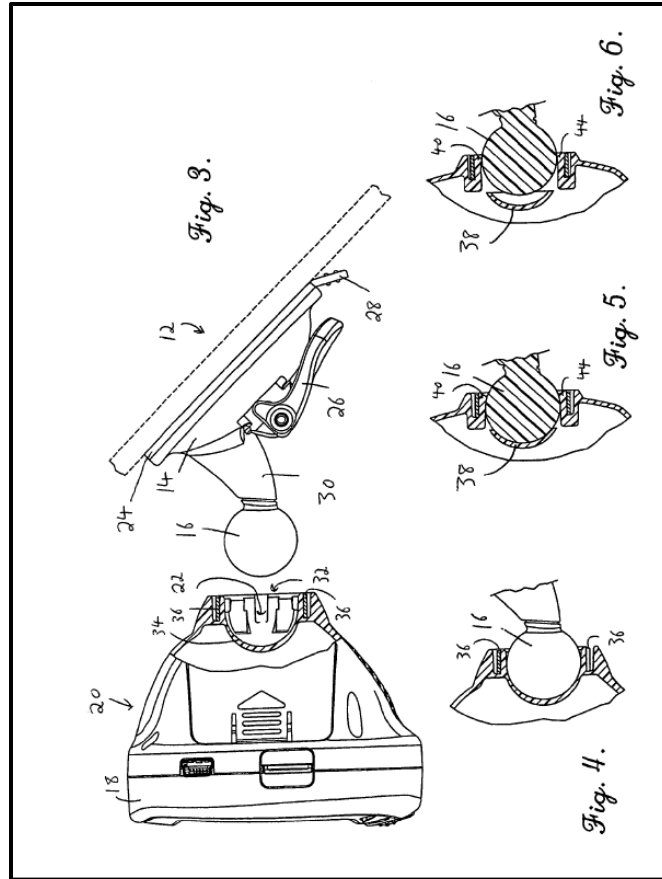


Figure 4. Sketch of an electronic device ball and socket joint mount (Kalis, 2007).

1.4 Hardware Research

1.4.1 NVIDIA Jetson

The Jetson Orin Nano, seen in Figure 5, is a compact AI platform from NVIDIA designed for a range of applications. Key specifications include a powerful ARM CPU, dedicated GPU, and support for various AI frameworks, making it suitable for tasks like robotics, edge computing, and machine learning. It consists of a 40-pin header and 4 USB 3.2 connectors. Pros of the Jetson Orin Nano include its affordability, energy efficiency, and robust developer ecosystem supported by NVIDIA. However, its cons encompass limited onboard storage and potential overheating issues under heavy loads. As for its

limitations, the Jetson Orin Nano might not be ideal for high-end, resource-intensive AI applications, and its smaller form factor may lead to compromises in connectivity options.



Figure 5. Image of the Jetson Orin Nano (NVIDIA, 2020).

2 PROBLEM STATEMENT

2.1 Problem Background

An intelligent robot must have some method of perceiving the world around it. In the case of robot vacuums, they must know the floorplan accurately while adapting to the changing environment around them. This mapping heavily relies on sensor positions and orientations. Additionally, the robot must make the most out of the multiple data streams from all sensors. With all this data, machine learning models can also be trained in situ given the robot has computational power and overhead. As consumer products brought to market must be permanent and robust in their configuration of sensors, a physical environment for testing these configurations prior to scale production is ideal and many

times necessary, especially in Tailos' case. In addition to the opportunity for testing sensor suites, Tailos would like to expand on sensing capabilities, whether this might be stair detection, human detection, or different conditions in different environments. The solution to achieving both wants is a universal sensor mounting platform, novel in the sense that Tailos' sensor suites are unique and effective for their application.

Thus, the problem is twofold. One being the lack of physical infrastructure for the potential variation of sensors, and two the lack of speed at which testing different suites can be done. Relative to the speed at which sensor suites can be tested, the team must develop a system whereby each potential sensor can be quickly added to the entire system and output useful data. With this, accurate mapping of sensor positioning becomes necessary. The entire system (software and mechanical) must work together.

Conclusively, Tailos requires a robust medium for testing variations of sensors. The senior design team aims to enable rapid sensor configuration testing while expanding the capabilities of Rosie—Tailos' flagship robot vacuum.

2.2 Problem Statement

With an expanded understanding of the problem that the team are trying to solve, the Tailos team come up with the comprehensive problem statement below:

*Design and implement a user-friendly mounting platform with the capability to
configure and evaluate robot sensor suites.*

3 REQUIREMENTS AND CONSTRAINTS

An effective engineering solution to the problem statement necessitates the presence of quantitative functional requirements in adherence to constraints. By translating the customer needs into a rigorous specification sheet, all design solutions including final deliverables can be developed and evaluated with respect to expectations via well-defined expectations.

In the scope of this project, a set of requirements and constraints were developed via a combination of direct statement by Tailos' engineers, visual and written descriptions of the overarching objective sought to be met and derived by examining their current product and technical stack. Figure 6 visualizes the customer needs regarding the visual coverage that a platform's sensor capabilities should provide.

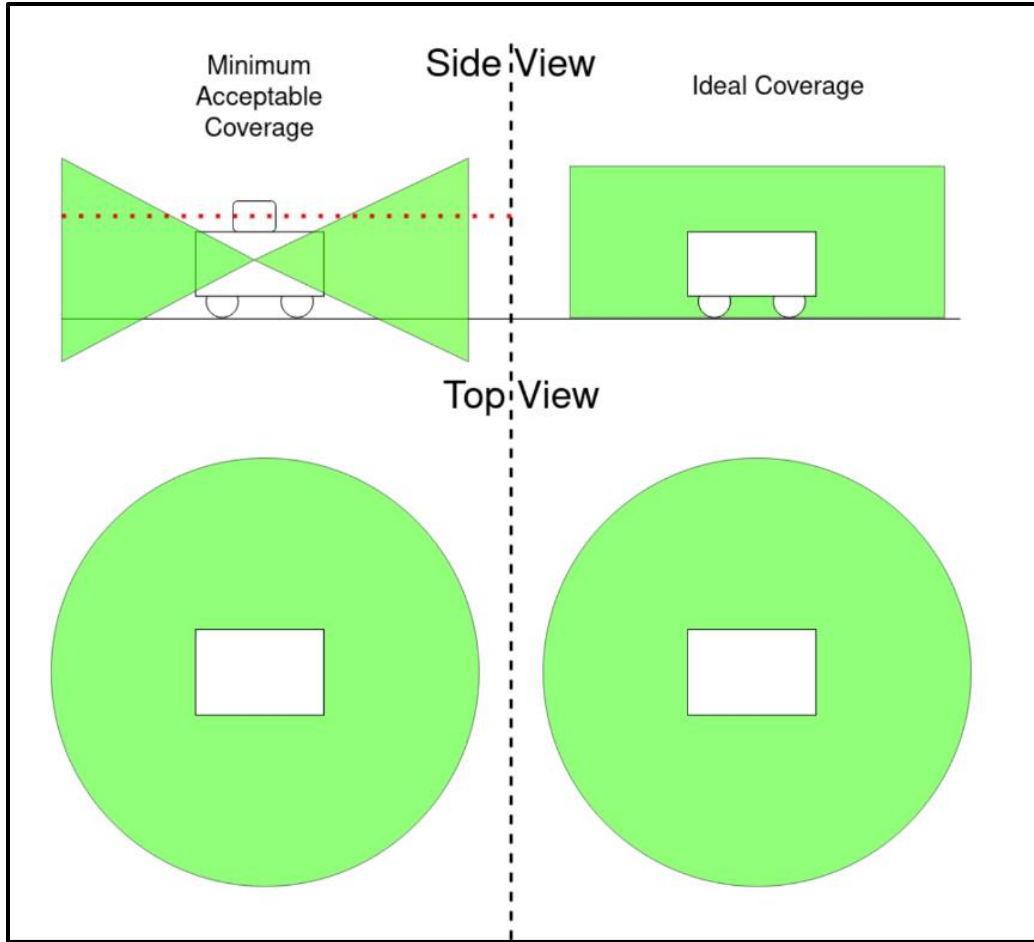


Figure 6. Minimum and ideal coverage (Tailos, 2023).

Due to the nature of these customer needs, translating them mandates that the functional requirements, expressed as demands, center heavily around the overarching concept of FOV metric. This FOV, both vertically and horizontally, must effectively match the provided image as shown in Figure 6, with the ideal case being complete coverage that subtends their current Production 1 (PD1) robot in its entirety. In addition, further information provided by Tailos about their current sensor suite and its limitations provided a solid quantitative baseline for defining a usable depth range to adhere to. Also, the platform's ability to enable different arrangements of sensor suites necessitates the presence of multiple degrees of freedom per sensor in terms of placement. These

placements should also be characterized by repeatability and stability under operation, which prompt the requirement to ensure accurate reporting of sensor position on a translational and angular basis along any degree of freedom whilst being subject to vibrational stability. Given that the platform is to be retrofitted onto the PD1 chassis, the robot's current performance and properties motivate the quantitative constraints the mechanical design and software stack must adhere to in fulfilling these requirements. These requirements and constraints are tabulated in Table 1.

Table 1. The Tailos team's specifications sheet.

| Demand/ Wish | Functional Requirements | Required Values/Targets | Units /Scale | Test/ Verification Method |
|-----------------|---|--|------------------|---|
| D | Vertical front & rear net sensor coverage (Field of View) | ≥ 70 (Front & rear each) | $^{\circ}$ | Imaging tests with tape measure in frame. |
| D | Usable net depth perception range | Max usable working depth ≥ 1.5 Min usable working depth ≤ 0.3 | m | Image resolution vs. working distance plots |
| D | Horizontal/planar net sensor coverage (Field of View) | 360 | $^{\circ}$ | Swept imaging across 4 quadrants |
| W | Degrees of Freedom of sensor position orientation | 5 | | |
| D | Linear Strafing velocity | 0.4 | ms^{-1} | Encoder wheel speed plots |
| W | Time to change sensor configurations | ≤ 30 | min | |
| W | Battery life | ≥ 1 | h | |
| D | Sensor translational position accuracy | ± 1 | mm | |
| D | Sensor rotational position accuracy | ± 1 | $^{\circ}$ | |
| Demand/ Wish | Constraints | Required Values/Targets | Units /Scale | Test/ Verification Method |
| Geometry | | | | |
| D | Mass of mounting platform with Robot | 10 | kg | Weight scale |
| D | Planar dimensions of mounting platform | $\leq 515 \times 250$ | mm | |
| D | Mounting platform height | ≤ 200 | mm | |
| Forces | | | | |
| D | Vibrational stability | Damping ratio (ζ) > 1 | | Accelerometer (look into modal analysis) |
| Costs | | | | |
| W | Manufacturing cost | ≤ 300 | \$ | |
| W | Project cost | $\leq 3230 + \text{PD1 chassis}$ | \$ | |

3.1 Requirements

Figure 6 provides the necessary information to directly deduce several of the functional requirements as it pertains to vision coverage, which are then outlined in Table 1. A circular sweep as shown from the top is simply a 360° in the robot's horizontal plane. This functional metric is satisfied by taking repeated images across each quadrant and viewing them for confirmation.

The vertical front and rear coverage were derived by using simple trigonometry under several conservative assumptions based on Figure 6 and the provided max height constraint of the retrofitted sensor mounting platform at 200 mm. The assumption is that the reference point, where the FOV is defined, is placed the robot's center of mass horizontally and vertically. Furthermore, the second assumption is that a vertical FOV must at least cover the very top of the mounting platform to the bottom of the chassis hardpoints where the wheels are attached. A calculation based on the provided computer aided design (CAD) file dimensions results in an FOV of 70° or greater, with the ideal case being 90° . This metric is evaluated by using images at a known distance with a tape measure to provide a known vertical coordinate system in physical units rather than relying on pixel resolution. By referencing an image with a vertical height shown in frame, an effective FOV can be calculated with basic geometric data. It is important to note that an overall vertical FOV is the sum of the FOVs of each sensor in use.

In terms of the usable net depth range, these functional requirements were derived by examining the current sensor limitations provided by the Tailos sponsors. Sensor noise limits the maximum working range of their RealSense D435 camera to be at 1.5m, so the functional requirement necessitates meeting or exceeding this value. Moreover, due to the

limitations of stereo matching when up close, the minimum working distance is reported as 0.3m, creating a blind spot in the interval of distances smaller than this minimum value, geometrically resulting in the subtended FOV resembling a frustum. Therefore, a sensor configuration supported by the platform must enable a minimum depth of at least less than 0.3m to mitigate the presence of blind spots.

A document of 5 sensors to be evaluated in conjunction with adjustability in each sensor itself results in 5 degrees of freedom that must be supported by a mounting platform design. With each degree of freedom, Tailos has explicitly stated that the accuracy of each position is to be accurate to 1 mm or 1° and the software to be developed for integrating the sensors must keep track of these position values.

Battery life and the time needed to change configurations were decided upon over a meeting and is expressed as a wish rather than a priority demand. Finally, the software needed to support actuator and sensor input/output must ensure that vehicle speed operates at the current status quo of 0.4 m/s, a balance between maneuverability and a speed low enough to allow enough time for the robot to detect obstacles. This speed is monitored through generated data plots by accessing the encoder values and the kinematic model of the mecanum drivetrain to ensure this requirement is met.

3.2 Constraints

The constraints are best characterized by considering that the mounting platform and software are to be retrofitted on the PD1 robot chassis provided. As a result, geometric constraints can be rigorously defined. It is explicitly stated by the sponsor that the platform weight with all the sensors must be no more than 10 kg, and that the dimensions of this platform to be no greater than the planar length and width of the robot from the top,

revealed by CAD at 515 x 250 mm. To ensure that the platform stays within the height footprint of future robot iterations while also providing room for sensors, the vertical height of the platform is strictly no greater than 200 mm.

In terms of force-based constraints, the need to maintain vibrational stability while the vehicle is moving with operational impellers is aimed at mitigating sensor noise and deviation of a sensor from its selected position or orientation. To avoid an arbitrary oscillation dimension from being used which can be too strict or too relaxed of a metric, a unitless damping ratio (ζ) is used as it can be used for all sensor mounts experiencing any type of vibrational mode. All sensor mounts must adhere to $\zeta > 1$, indicating that the system must be critically damped at the least. This metric ensures that the mounting platform is designed and prototyped with damping strategies in mind and can be evaluated with empirical experimental data by using an accelerometer when the platform is subject to vibration, whether by impact or motion. It is important to assert that vibrational stability limits the range of solutions and is thus a constraint on any system rather than a functional requirement.

Finally, the budget motivates the cost-based constraints, where the material costs used in manufacturing the platform are valued are set at \$300 by agreement with the sponsor over a meeting. The cost of the sensors and microcontroller are valued at a total of \$2920, which is then added to the material costs and PD1 chassis cost, yet to be provided, to provide a grand total project cost for providing all deliverables.

4 DELIVERABLES

4.1 Specific Deliverables

Team Tailos' final mechanical deliverables will include a modular sensor mounting platform that is reproducible based on the needs of different sensor suites provided by the sponsors. This will be presented to the team in the form of a CAD model as well as a physical construction to be mounted on an existing robot platform. The platform should account for a range of sensor FOV and maintain modularity to the extent that each FOV can be accommodated. Along with these, the team will deliver a collision analysis of the system.

On the software side, the team will deliver a repository of the code needed to move the robot and activate the sensors and cameras. Also, the team will present the vibrational analysis of the system when the robot roves around.

4.2 Cost Estimation

When speaking to the sponsors of this project, the senior design team proposed a budget of \$300. This is an initial assumed value variable on evolving tasks and deliverables over the project. All these funds will be used during the manufacturing phase of this project due to the team already acquiring CAD software through the UT Austin and embedded software being free.

The software and hardware deliverables include the integration of an Nvidia Jetson Orin Nano with the robot's existing embedded systems. These systems encompass each individual mecanum drive wheel, existing permanent sensors, and most other tasks run by the existing PCBs.

5 MECHANICAL DESIGN

The mechanical design of this project includes multiple phases, seen on the Gantt chart in Appendix F, with Phase I being Idea Generation, Phase II being Idea Selection, and Phase III being Design. Specific design methods, such as functional modeling, morphological matrices, and Pugh charts were used to systematically generate and select the best design. The following subsections go into detail on these methods.

5.1 Mechanical Idea Generation

For Phase I of this project, the team systematically generated ideas with a method called mind-mapping, then organized these ideas in a morphological matrix to create full designs. First, the team focused on the main problem and the main function for the system. This is an important first step to start idea generation because it focuses the teams brainstorming on how to solve the given problem. Some questions that are generated from this are: What are the inputs and outputs of this system? What is the main function of this system? Can the team dismantle this main problem or function into different individual problems or sub-functions? It was necessary to conduct functional modeling to answer these questions.

In Figure 7, a black box diagram was created to display the inputs and outputs of this function. The arrow with a solid line on the top of the box shows the energy input and output of the system. Electrical energy (EE) from a battery is the input, then heat and noise from the DC motors and light from the cameras and lidar are the energy outputs. The middle double lined arrow represents the material input for the system. Here, sensors are the main material that provides feedback for evaluation. Lastly, the dotted line on the

bottom of the diagram is the information input and output from the system. The input information is an on and off switch and the output is the sensor/camera converge of an area. A monitor will output this coverage and the robot speed for a visual information display.

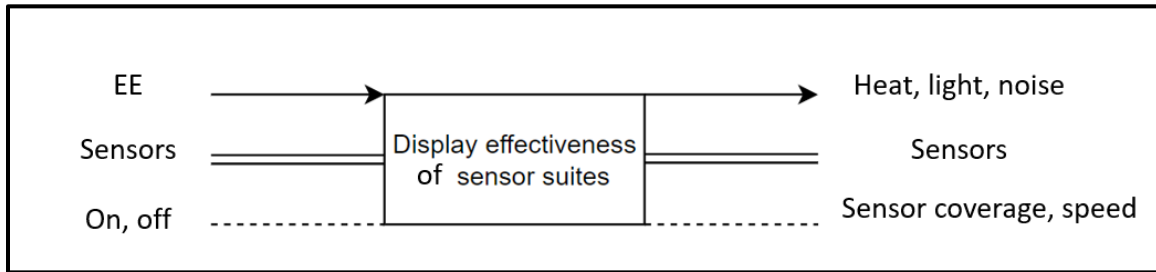


Figure 7. Blackbox diagram of the sensor mount system.

Continuing along with the functional modeling, a functional tree of the sensor mount system was created (Figure 8). From the main function of the system, multiple other functions split into a branching structure. The main subfunctions were “control movement,” “mount sensors,” “protect electronics,” and “evaluate sensors.” Controlling the movement of the robot and evaluating the sensors are more suited for the electrical and software design of this project and so the mechanical sub team will only explain “mount sensors” and “protect electronics.” The functions that split from “mount sensors” are “stabilize sensors” and “position sensors.” These two functions are important for how the sensors will be positioned on the robot and what kind of design will hold these sensors in place. The next main subfunction for this system is how the electronics will be protected. This entails securing the Jetson and dividing the sensors into different ports.

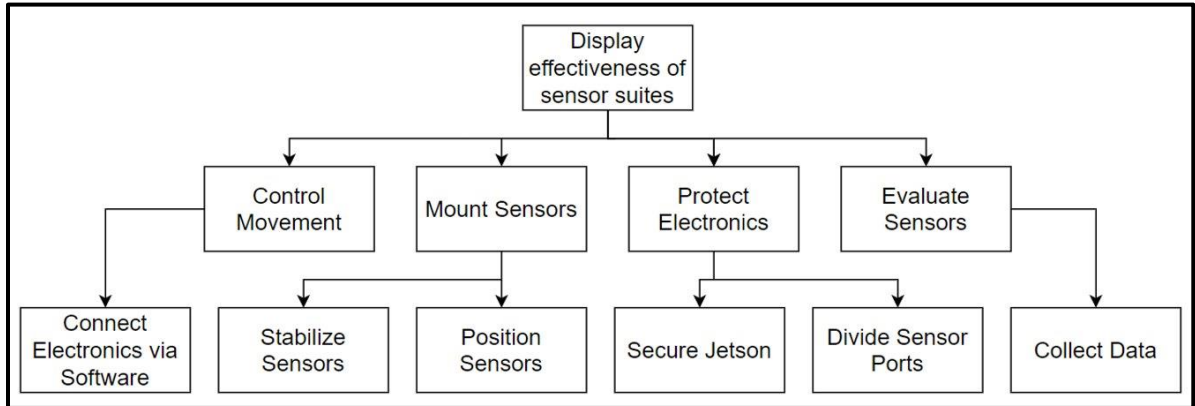


Figure 8. Functional tree of the sensor mount.

The method used to generate ideas was conducting a mind-map exercise seen in Figure 9. In the center of this node-like structure, the main function was written, which the team then brainstormed different solutions to the selected subfunctions. The solutions for the “stabilize sensors” function were using either an optical table type design, a magnet grid, and a carbon fiber tube or aluminum extrusion frame. The optical table design is a plate with holes throughout it as designated spots for fasteners to mount the different sensors. Next, the magnet grid idea uses the magnetic force between two plates to secure the sensors. Another idea is the carbon fiber tube design which utilizes tubing as a frame around the outside of the robot footprint. This frame allows for multiple layers lying on top of each other for more mounting positions and basic height adjustment. Finally, the aluminum extrusion idea is like the carbon fiber tube design, yet this idea will utilize extrusion columns for an extrusion frame’s height adjustability.

Next, the team focused on the “position sensors” function. Some of the basic mounting forms were inherent to which platform or frame the team previously brainstormed for the “stabilize sensors” function. The rectangular platform mounting is the type of mounting

the optical table possesses. Direct mounting with fasteners will hold sensors and cameras perpendicular to the table's top surface. The rectangular beam mounting type will use T-slots for easy mount fastening on the four sides with these channels. This type of mounting allows for linear movement along the channel as well, which is a satisfactory solution to increase the number of mounting positions. Next, a more unique idea that emerged is using a ball and socket type joint for an increase to the number of degrees of freedom for a sensor. This type of mounting is inspired by Figure 4, the electronic device ball and socket joint mount diagram.

The team then looked at solutions for the “divide sensor ports” subfunction. A universal serial bus (USB) hub is the only solution to achieve additional ports for sensor input, so mounting this hub is the true focus of the solutions. Two ideas came to mind, one being mounting the USB hub on the Deutsches Institut für Normung (DIN) rail on spots around the Jetson or directly mounting the hub onto the Jetson securing plate. DIN rail is used universally with electrical component mounting and is a great solution to keep the USB hub modular though it is an extra original equipment manufacturer (OEM) part that does not mesh well with sleek designs. The other option of mounting the hub to the Jetson securing plate allows for fewer parts but lacks modularity.

The final subfunction the team focused on was “secure Jetson.” The two solutions that the team conceived were either positioning the Jetson in the middle of the robot or in the back. Positioning the controller in the middle reduces the ease of placement but allows for better lidar coverage and vice versa for the back position.

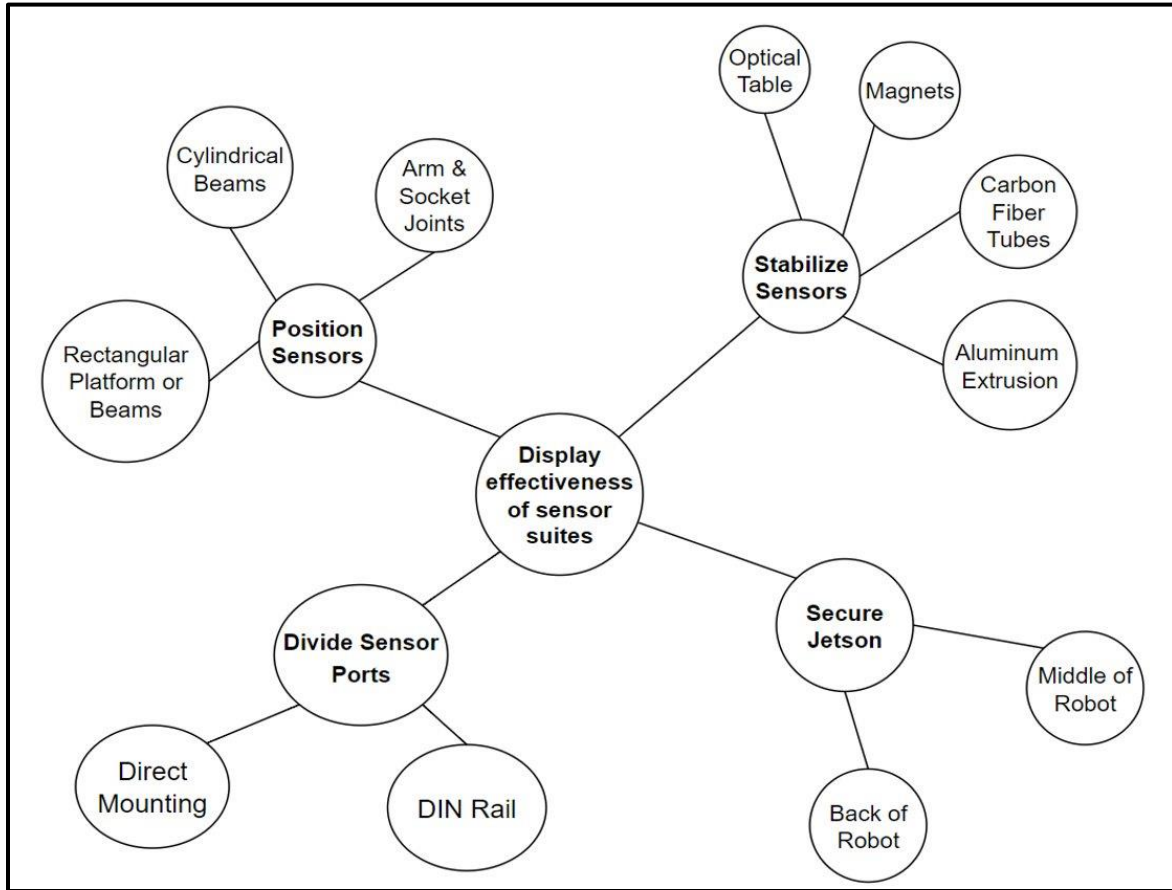


Figure 9. Image of the sensor mount mind-map.

Table 2 shows the morphological matrix, a method used for combining different individual features to present a fully realized design. Four of these matrices were constructed in Appendix B.

Table 2. Morphological matrix table.

| Subfunction | Solutions | | | |
|---------------------|----------------------|-------------------|----------------------|--------------------|
| Stabilize Sensors | Optical Table | Magnets | Carbon Fiber Tubes | Aluminum Extrusion |
| Position Sensors | Rectangular Platform | Cylindrical Beams | Ball & Socket Joints | Rectangular Beams |
| Secure Jetson | Middle of Robot | Back of Robot | | |
| Divide Sensor Ports | DIN Rail | Direct Mounting | | |

To start the full designs, the team combined the optical table feature, the rectangular platform, the middle of robot position for the Jetson, and the direct mounting of the USB hub. Figure 10 below shows the sketch of this design. The blue portion of the image is the optical breadboard with its many holes for fasteners. Not shown is the Jetson enclosure which is underneath the breadboard. This design will be elevated with brackets above the maximum height of the frame to give the Jetson's cooling system more space to properly exhume warm air.

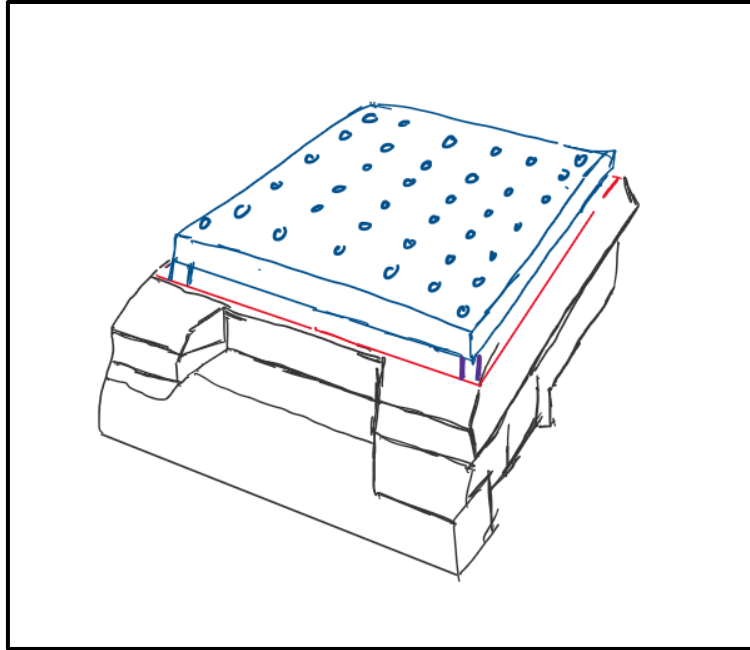


Figure 10. Sketch of the Optical Table design.

Below is Figure 11, a sketch of the Magnet design. The blue portion is a grid that is graduated to have precise sensor adjustments. The team also combined the ball and socket mounting design which allows for three degrees of freedom positioning for the sensors. This design utilizes the back of robot Jetson positioning and DIN rail mounting for superior access and modularity for the controller and sensor divider.

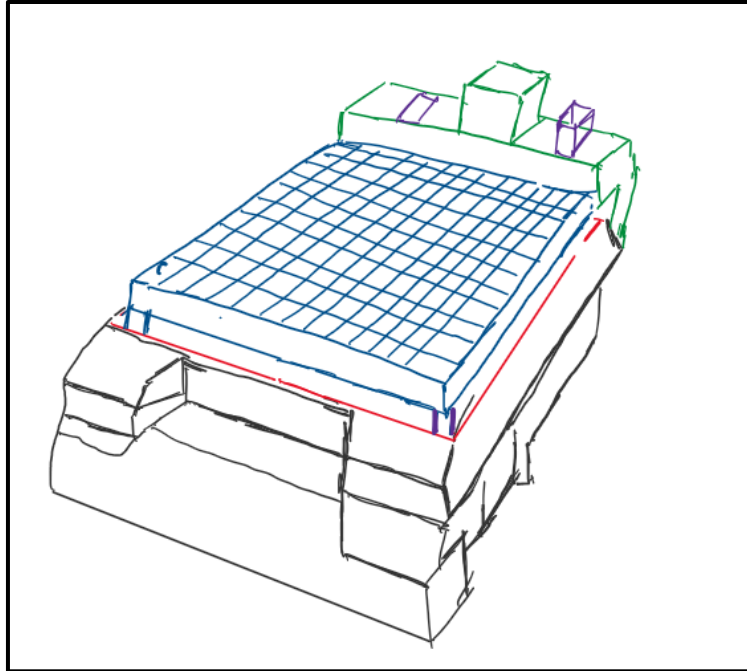


Figure 11. Sketch of the Magnet design.

Below is Figure 12, which are images of the carbon fiber tube design. This design combined the carbon fiber tube frame, the cylindrical beam, middle of robot Jetson position, and direct mounting of the USB hub. The frame is completely modular with lugs that support the entire system to a fixed plate that came with the robot model. This design allows for one degree of freedom in the roll direction.

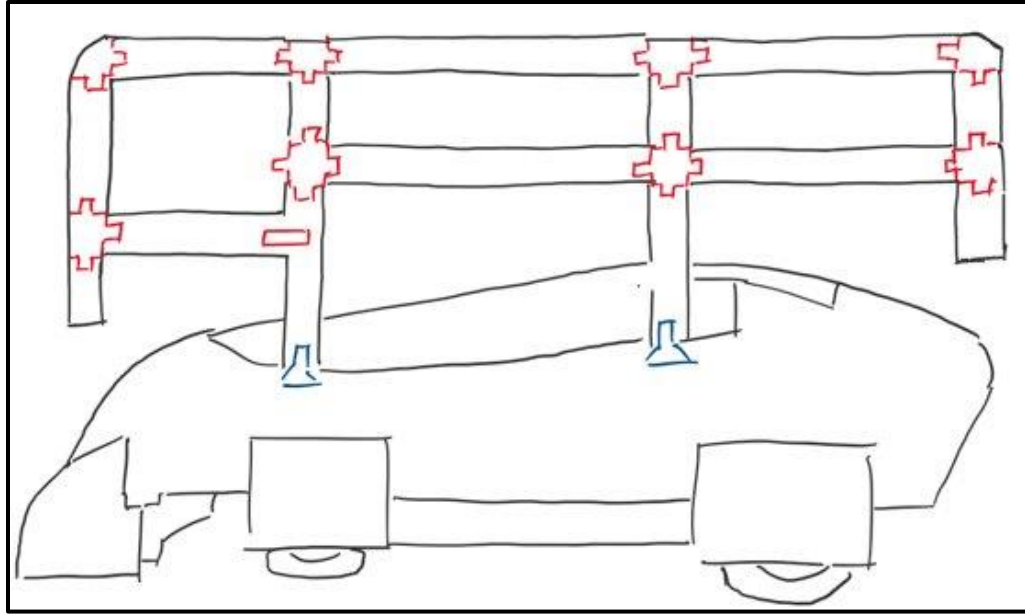


Figure 12. Carbon fiber tube side view.

The design shown below, Figure 13, is a model of the first mounting platform iteration which makes use of aluminum extrusions and integrated mounts that repurpose existing holes on the Tailos bot. Two key issues with this design are the lack of geometrical integration and the extension of the robot footprint. Reviewing this iteration with the Tailos team they had mentioned a desire for integration with the existing panels. Additionally, the team mentioned an unnecessary extension of the robot footprint with aluminum extrusions that sit further than the existing perimeter of the robot, as shown in the figures above.

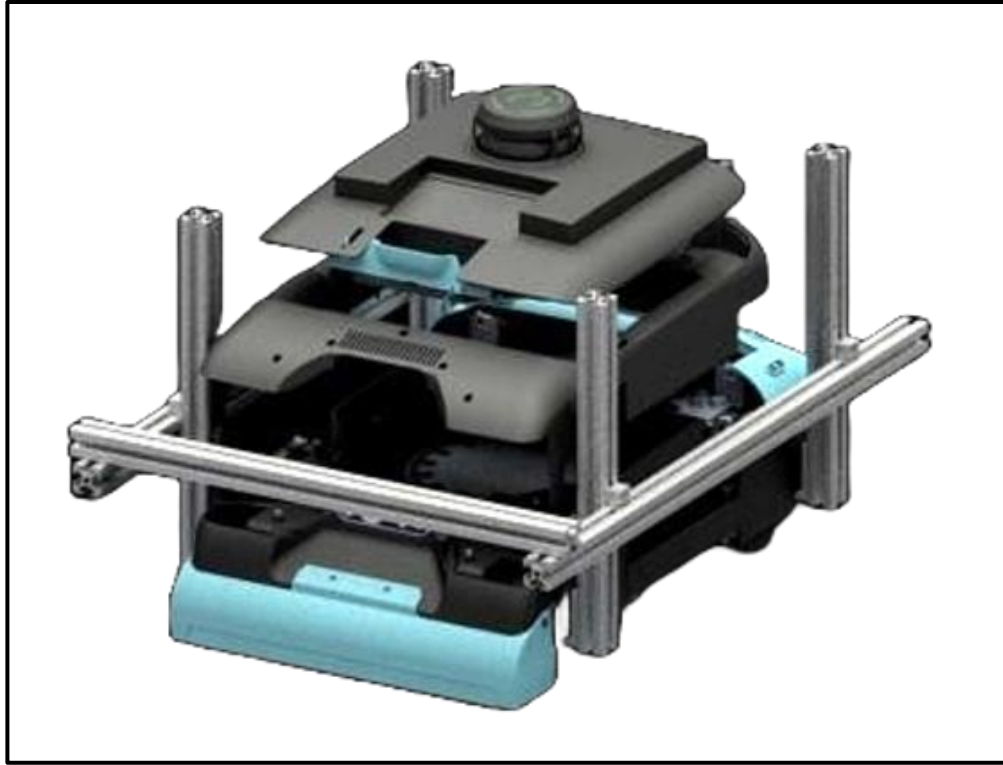


Figure 13. Aluminum extrusion design

5.2 Mechanical Idea Selection

After completing the Idea Generation phase of this project, the selection of a main design was done with a systematic method called the Pugh chart. Different criteria of the designs were evaluated using Back of Envelope (BOE) calculations. The criteria include mass, cost, number of degrees of freedom, number of mounting positions, customers' preferences, and ease of access/mounting.

Data sheets found on the vendors websites (McMaster-Carr and 80/20) were used to make these calculations. These data sheets are seen in Appendix A and all the BOE calculations can be seen in Appendix D.

Firstly, the dimensions of the materials needed to be established the calculations. The selected carbon fiber tubes have an outer diameter of 0.610 in and inner diameter of 1/2 in. These dimensions were selected due to being a good diameter for a rigid mounting

mechanism. The 40-4040-Lite aluminum extrusion was selected due to the dimensions being a medium size for a more compact design allowing for more mounting positions. Moving on to the optical table design, the robot footprint is the assumed maximum platform length and width which is also the same for the magnet design.

After doing basic volume, mass, and cost calculations, some of the geometric characteristics of the designs needed to be analyzed. The number of degrees of freedom for the designs were imagined with engineering intuition by visualizing how the mounting designs would rotate in 3D space. Along with these visualizations, total mounting positions were calculated by assuming the mounting interface for all the designs would be a 20mm x 20mm square. This constant allowed for proper comparison between the distinctive designs.

The ease of access/mounting can be described as the number of steps it would take to mount a sensor or camera to the design. The optical table takes multiple fasteners to attach and detach sensor, four steps. The aluminum extrusion and carbon fiber tubes would only take one step each. For the aluminum extrusion, the user can easily just slide the sensor mount from the exposed side onto the channel. Additionally, for the carbon fiber tubes, the sole step would be securing a shaft collar type mounting interface that only needs one fastener. The magnet design is easy as well, with the user just placing the mount onto the plate for easy attachment.

Finally, the customer preferences were the final criteria the team analyzed. The team evaluated the preference as either being a like or dislike (1 or 0). The sponsors liked the aluminum extrusion and optical table designs but disliked the carbon fiber tube and magnet design. Later, the team learned that the carbon fiber tube and magnet designs were disliked

due to lack of aesthetics, unnecessary complexity, and damage to the sensors with magnetic fields hovering around.

The Pugh charts, seen in Appendix E, show that the carbon fiber tube design was the best out of all the other designs with its modest number of degrees of freedom, an enormous number of mounting positions, how light it is, and its ease of access/mounting.

After the team systematically selected the carbon fiber tube design, the sponsors decided to change their requirements. One of the things they wanted to do as a company was move away from injection molding, which was the main way of manufacturing the Rosie models. They required a “sleek” design which consisted of nice curves and a black color scheme. Also, they required most of the parts and assemblies to be manufactured using additive methods such as 3D printing with FDM printers. The carbon fiber tube design did not meet these requirements, so the team needed to completely change the design and focus on the customers’ preferences instead of the Tailos team’s own methodology. The next section describes the new design in detail.

5.3 Final Mechanical Design

After Phase II of the design process, as stated earlier, the sponsors presented a change in mechanical design requirements for the project. The design team was made aware that this was not meant to be a pure R&D platform, and that topological integration with the existing platform was more important. This necessitated a lesser need for sensor positioning resolution, as considering the existing platform’s design for injection molding (including thin walls, drafted panels, and ribbing that would be excessive and unnecessary for additive), integration in many cases brings less opportunity for variability in placing

sensors. A specific requirement disqualification from the Tailos team was the no longer imperative height adjustability for each given sensor.

Below is Figure 14, an image of the final position and design of the Jetson enclosure. This is a two-body design for 3D printing, with the bottom portion consisting of multiple direct mounting positions for the USB hub and Arducam board, both being able to move to either side. The enclosure is open on the walls to allow for ease of access to the different ports on the Jetson. There are built-in standoffs that have holes in them for heat set inserts to be placed which fasten the Jetson controller onto the enclosure. The second body, being the top cover of the enclosure, is fastened to the bottom body via bolts that are secured to heat set inserts. This design is simple with not many OEM parts.

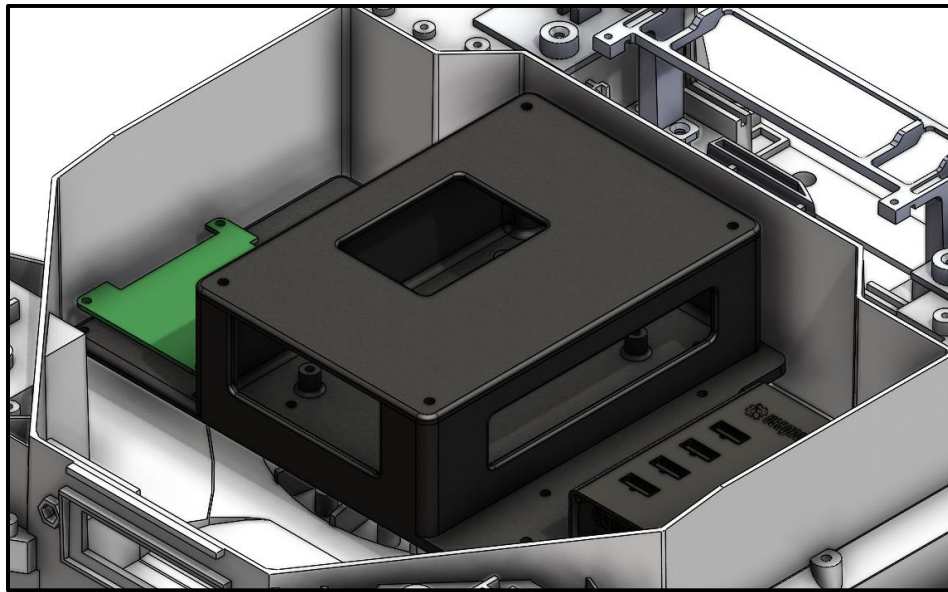


Figure 14. An image of the Jetson enclosure.

Below, Figure 15, is a snapshot of the sensor mounting platform with two examples of sensors (Arducam) mounted and angled downwards to show a potential sensor suite scenario. As shown, the back portion of the two-part sensor mount slides into the panel that is attached to the robot. The upper-level pegs with visible M4 holes are used to mount the

back piece of the sensor mount with hardware to keep the entire system secure and in place. The lower-level pegs are used to mechanically lock the lateral movement of the sensor mount using the curvature of each rib and the nature of the spacing between each rib. The 3-rib back mount sticks out far enough to allow the second piece of the two-part system to have rotational freedom as much as is necessary.



Figure 15. An image of the perimeter mounting solution.

As you can see below in Figure 16, the mounting mechanism operates in a similar way to a GoPro mount, allowing rotational variability and the ability to lock with hardware. The version above is an alternative mount that the design team developed which allows the user to mechanically choose a certain degree of rotation prior to locking the entire mechanism in place with hardware (M4 bolt and nut). The innermost rib on the bottom part of the mounting system has extruded triangular geometry which behaves like a gear when met with the top part (that has cut-out triangular geometry). When sliding the top part into the bottom part the entire mechanism will 'click' into place. Rotation by the user will result in

subsequent 'clicks', each at a 45-degree increment. This entire model was parametrically developed by the design team, so any necessary change to the degree increments can be made by adjusting a single dimension.

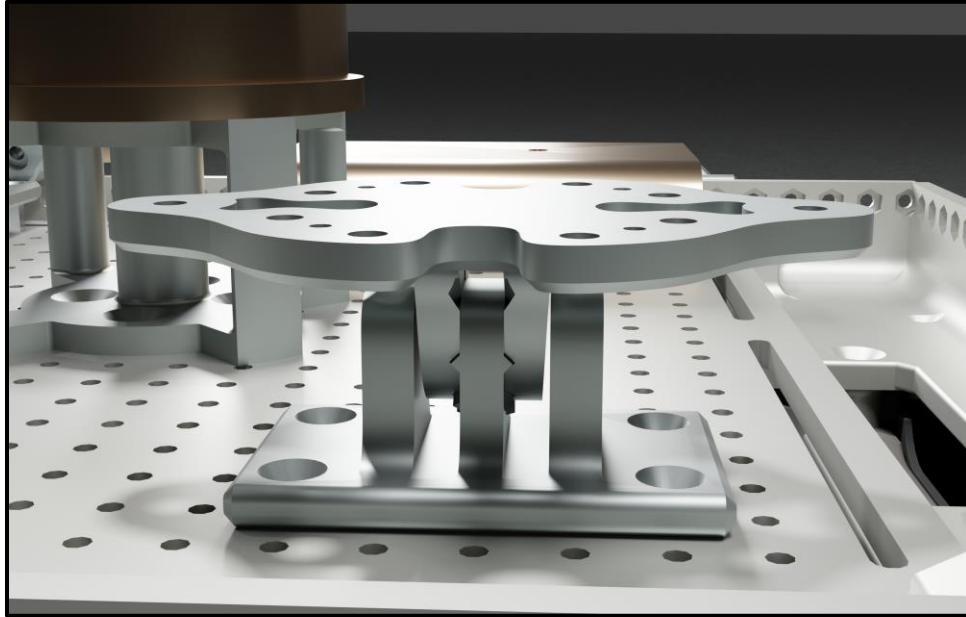


Figure 16. An image of the V2 degree-ratcheting mount.

With the new sensor mount mechanism, the design team was able to reintroduce the possibility of multiple degrees of freedom when mounting each respective sensor to the robot. Shown above are two sets of mounts that attach to each other (in this case perpendicularly), to allow for two axes of rotation. So, for example, in the case where a sensor needs to be mounted more within the footprint of the robot than allowed for by the perimeter mounting solution shown below in Figure 17, a system of mounts can be attached to one another and mounted at the base to the central optical table, at which point the sensor can be axially rotated to face outward and perhaps flush with an outer surface of the robot footprint.

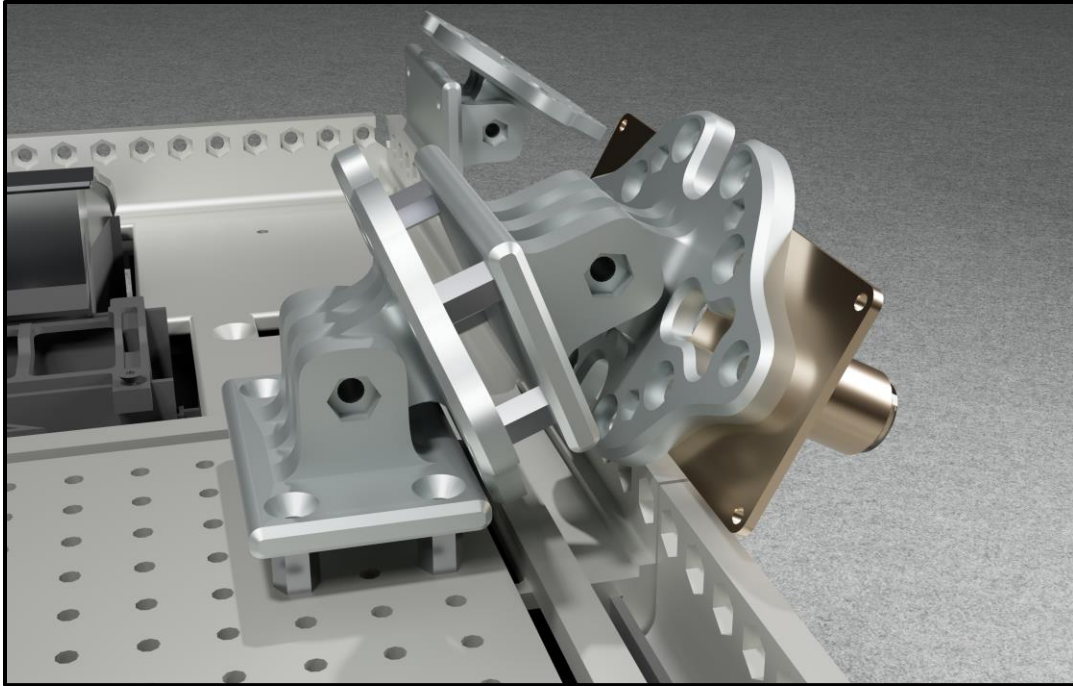


Figure 17. Image of a sensor mount combination.

The centrally mounted optical table is shown in the rendering above. The bottom side of the optical table contains counterbored hexagonal geometry to insert M4 nuts as well as four counterbored 4mm holes to insert permanent magnets. Magnets are inserted into the panels as well to mount the optical table with the entire sensor mounting system. A vertically restrictive extrusion is included in the panels as well to ensure the optical table stays in place. One potential issue brought up by the sponsors is unwanted flex in the optical table from the placement of sensors in combination with robot movement. A solution for this which has been incorporated into the design is extra support for the optical table included in all portions of the panels which are directly below the optical table. In addition to this, a version of the optical table with cross-sectional ribbing on the underside has been delivered as well.

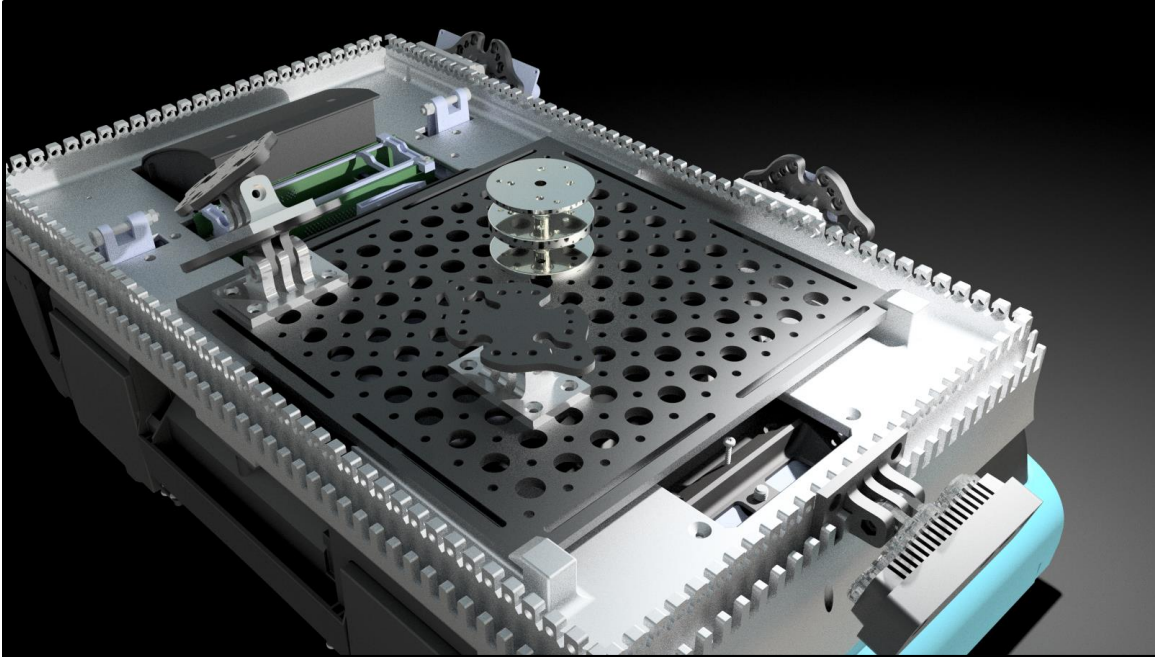


Figure 18. Rendered view of optical table design.

Much of the interfacing between the team's panels and the existing robot is done with existing mounting holes. Some of these holes include a threaded shaft upon which an M4 nut would sit to secure outer panels onto the robot subframe, and others include a threaded hole that takes a flathead screw. In addition to panel geometry which sits flush with the interface of the threaded hole, the team has purchased longer flat-head bolts to ensure a correct fit.

As for interfacing with the sensor mounting platform, the sponsors suggested using thread-forming screws and 'drill-size' M4 holes for the initial iteration, where panel fitment and topological discrepancy are being tested/iterated more so than the inherent function. These thread-forming screws were used for the first physical iteration, after which threaded inserts for plastic were used for prototypical permanence.

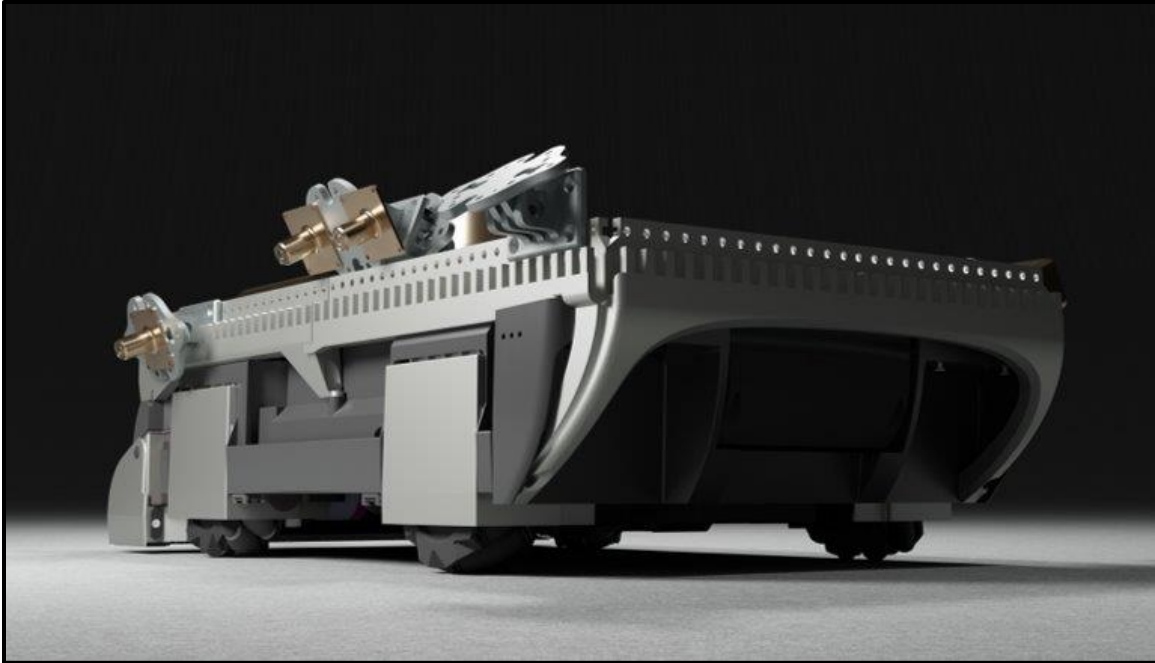


Figure 19. Image of the quarter panel integration.

Additionally, the entirety of the team's mechanical system has been designed parametrically, whereby certain dimensions are relevant to other dimensions, and sketch constraints are used where necessary. This allows quick changes to be made to the model by looking into the model's history and adjusting dimensions of interest. Effectively, dimensional changes no longer get in the way of the model's function, and geometrical debugging becomes much less of an issue. As a deliverable, this means the sponsor has ease-of-use in changing dimensions for future iterations, whereas many CAD models might not have this inherent functionality (Bhooshan, 2017).

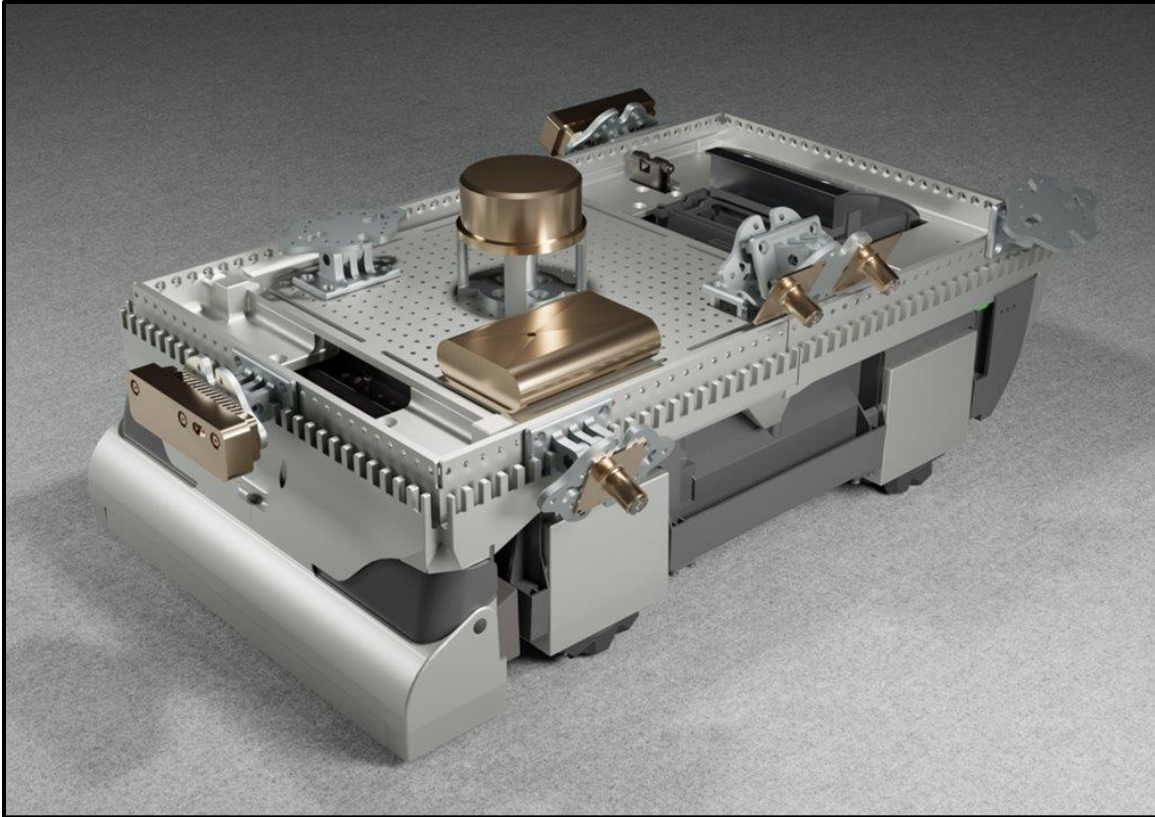


Figure 20. Rendering of Sensor Suite Platform assembly w/ mock sensor suite

6 SOFTWARE DESIGN

The software design methodology for this project is mostly guided by the sponsor. Since the software design centers around replacing the current IMX8 microcontroller with a Nvidia Jetson, the software should be compatible with the sponsor's current codebase and workflow. This involves developing in the same environment. Specifically, this involves the Linux Ubuntu 22.04 LTS operating system, version of Robot Operating System (ROS) 2 Humble, and codebase distribution with Docker containerization.

6.1 Software Decisions

The first stage of the project was oriented around workflow and codebase management. This project aims to integrate the current robot functionality onto an NVIDIA Jetson Orin Nano board. The team learned ROS2 along with Jetson GPIO pins. ROS2 is an open-source software framework featuring proprietary, cutting-edge robotics applications and packages that are widely used in industry. At first, the software team programmed the Jetson directly by connecting to a monitor and user peripherals. This workflow posed major workflow bottlenecks, especially once the Jetson was mounted onto the mobile robot. As a result, the team explored remote protocols such as VNC and remote desktop; however, these graphical remote interfaces were not well-supported on the Jetson. The Tailos team considered SSH protocol; however, the team's deliverables involved graphical simulations that would not be compatible with SSH. After the first meeting with the team's faculty advisor, the team learned that development on the Jetson is mostly on a remote machine that updates a codebase repository. The Jetson then pulls from that repository to update the robot software. In the end, the team remotely accessed the Jetson via SSH, a popular command-line interface protocol to update it as needed and performed graphical tasks on the team's own Ubuntu machines instead of the Jetson directly.

For the sponsor, the team must also work in a Docker container for two reasons: the ROS2 framework is only supported in a Docker container for the Jetson, and the software along with the environment it operates in must be packaged in a Docker image that can be distributed scalably and seamlessly (Open Robotics, 2023). As such, the software team currently adopts the following workflow:

1. SSH into the Jetson, provided the Jetson is connected to a network (ethernet or wireless)
2. Run a custom script to set the embedded interface on the Jetson (GPIO pins, low-level optimizations, power settings)
3. Run the Docker container to use the ROS2 framework
4. Clone the Tailos repository that is updated and developed on a separate development machine
 - a. Software development can still occur directly on the Jetson for debugging and minor changes
5. Build the ROS2 packages and run nodes accordingly

When interfacing with all four motors, the Jetson only offered three PWM pins (NVIDIA, 2022). To address this issue, the software team procured an external PWM driver board that communicates via the I2C protocol. Currently, software and embedded teams are working on teleoperating the robot with a kinematic model in ROS2. Concurrently, the software team is also integrating the software design process following the extreme programming paradigm in which sponsor feedback on software design is emphasized and iteratively solicited (Raeburn, 2022).

6.2 Electrical Hardware & Software Execution

With a scalable, solidified software development workflow, we've developed teleoperation functionality on the robot as demonstrated in Figure 21. On the hardware side, zip ties temporarily managed the cables with a breadboard terminal as the high voltage (12V) bus for the robot.

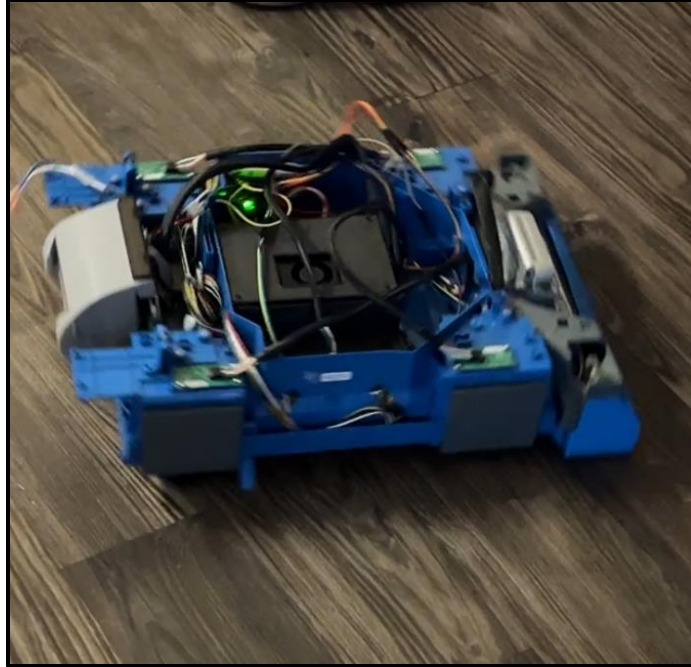


Figure 21. Rosie spinning with Jetson teleoperation.

Currently, the team are developing the sensor evaluation suite that will be interpreted with RViz, a data visualization library in ROS2. The main objective of the sensor evaluation suite is to seamlessly reconfigure and calibrate sensors, log each configuration state with sensor types, and assess the overall performance of the configuration. The following black box model shows the key performance metrics such as coverage and FOV as a function of space.

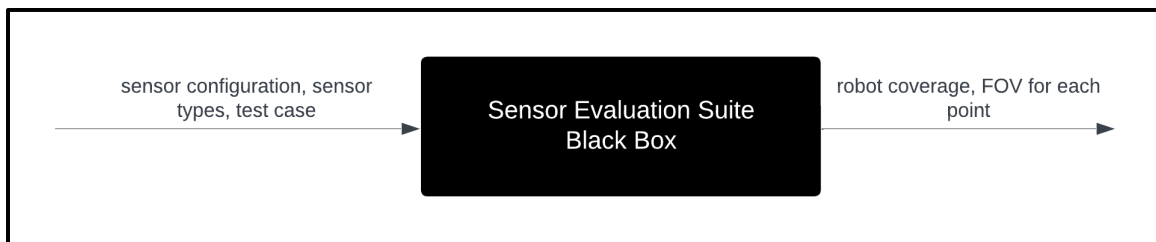


Figure 22. Black box diagram of the sensor evaluation suite.

Regarding the motor control side, the user can specify position control in the ROS2 framework with a teleoperation node that sends commands over a topic, `/cmd_vel`, that is

interpreted by the software on the robot in real-time as shown in Figure 23. The robot kinematic model acts as a black box for converting desired motion into motor velocity commands.

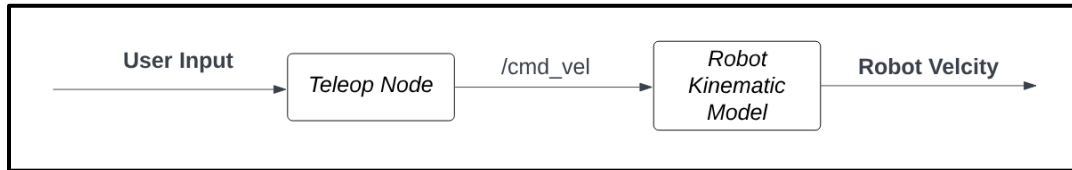


Figure 23. Black box diagram of the sensor evaluation suite.

Further behind the scenes, the position controller of the robot tracks a reference position, x_0 , that is manually specified by the user or by mapping algorithms. The position controller is a PID controller that sends velocity commands to the four mecanum wheels. The PID controller regulates the actuator velocity such that the encoder values read the desired displacement. A simplified block diagram of this position control is shown in Figure 24.

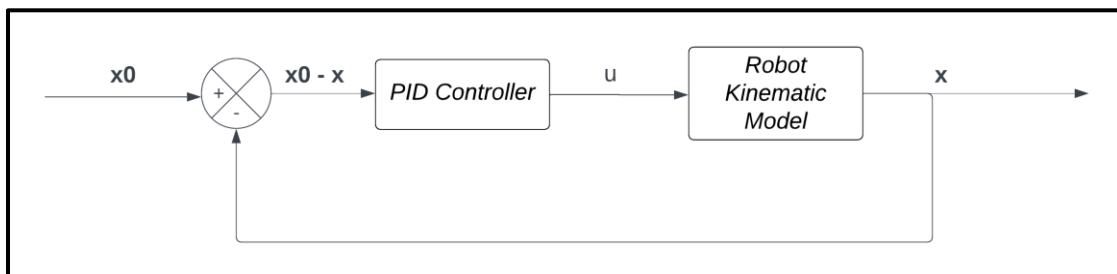


Figure 24. PID controller for odometry and robot position control

Lastly, the sensor integration requires prior documentation and interfacing with their respective API. The sponsor graciously provided the sensors the team is interfacing with time-of-flight (TOF), LIDAR, and stereo camera sensors that will help the robot map its environment in real-time.

7 RESULTS & ANALYSIS

The main result of this project is the physical prototype with all the quarter panels attached, mounts, sensors and cameras, and the robot is fully teleoperational. Along with this, to fully understand the strengths and weaknesses of the final design, the team conducted simulations and experiments. In this section, the team utilizes finite element analysis (FEA) of a universal mount colliding with a stiff object as well as a vibration study on the roving robot system.

7.1 Physical Prototype

Below, Figure 25, is an isometric view of the physical prototype. Like the 3D model, the quarter panels that allow for horizontal sensor mounting are on the top corners of the robot. One issue the team had when manufacturing these panels was the wait times for Raise3Ds at Texas Inventionworks. Due to this issue, one of the quarter panels is white, seen in the back right of Figure 25. The grey object in the middle of the prototype is the optical breadboard with the cylindrical lidar and ovalar TOF sensors mounted on top of it. On the front and left side of the robot, the universal mounts are secured to the quarter panels with the Arducam camera on the left and the Oak D on the front.

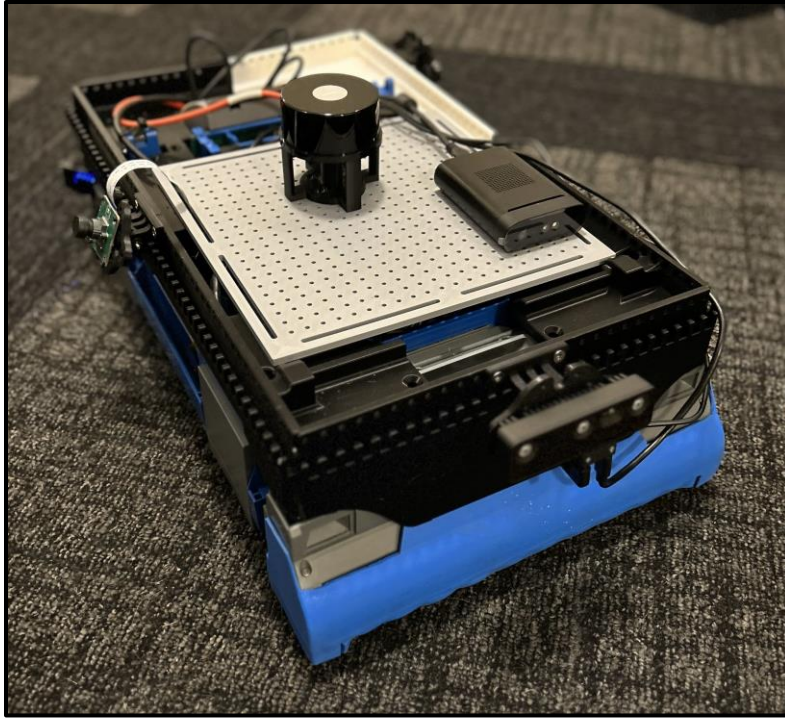


Figure 25. Image of the physical prototype.

7.2 Collision Analysis

To validate that the universal mount assembly is strong enough to take a head-on collision with a rigid body, the team conducted a collision simulation in SolidWorks. Below is Figure 26 which shows the stress results for the 23rd step of a Drop Test with a mount velocity of 0.4 m/s (this being the maximum velocity of the robot as stated by the sponsors) colliding with a rigid wall that is parallel to the mount face. 25 steps were split over a time span of 70 microseconds after the initial contact with the wall. The 23rd step is shown because the greatest stress concentration was found here. From the diagram, you can see that the maximum stress the mount experiences with these parameters is about 5 MPa. The stress-strain curve for PLA shows that this is a point in the elastic region which verifies that the mount will not permanently deform/fracture from a collision such as this (Shuhua, 2014).

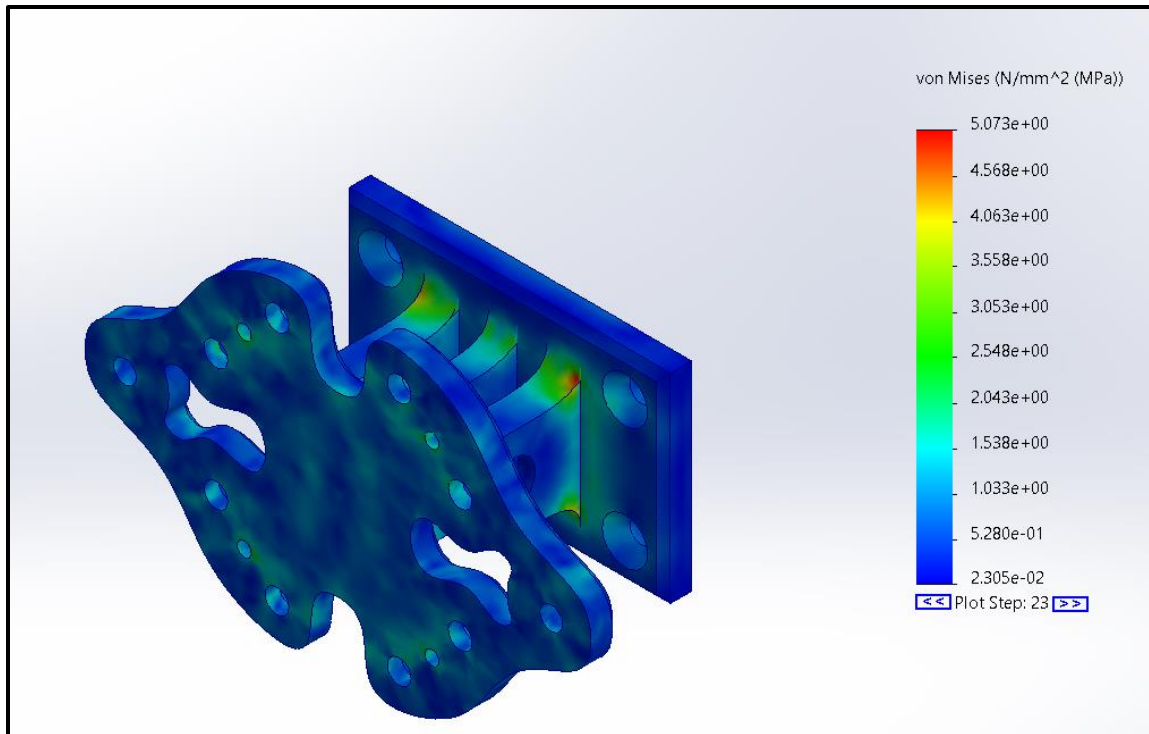


Figure 26. Image of the 23rd step of a universal mount collision FEA stress result.

7.3 Vibrational Analysis

The sensors must not only be mounted securely, but they must also withstand the mecamum drive vibrational dynamics to minimize sensor noise. The Tailos team gathered the data by mounting an IMU to one of the team's sensor mounts. Then, the team drove the robot forward at maximum speed. The IMU interfaces with an Arduino Uno that logs the data into the Jetson as shown below.

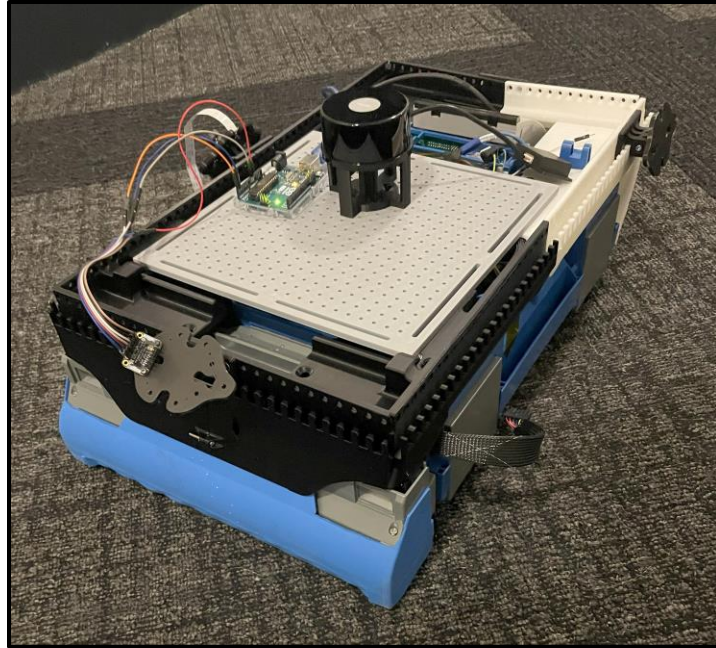


Figure 27. Vibrational measurement setup

The Jetson recorded the data with a Python script that also performed a vibrational analysis of the signal. Raw accelerations in the x, y, and z directions are shown in Figure 28. The acceleration signals across the board seem stochastic and very noisy, and the team likely believe this is due to the IMU undersampling since it was limited to 60 Hz; however, the team couldn't confirm higher frequency data since the team was bottlenecked by time and the team's IMU sampling rate. In the frequency domain, the fast fourier transform (FFT) of the raw data suggests broad frequency content or undersampling of the data.

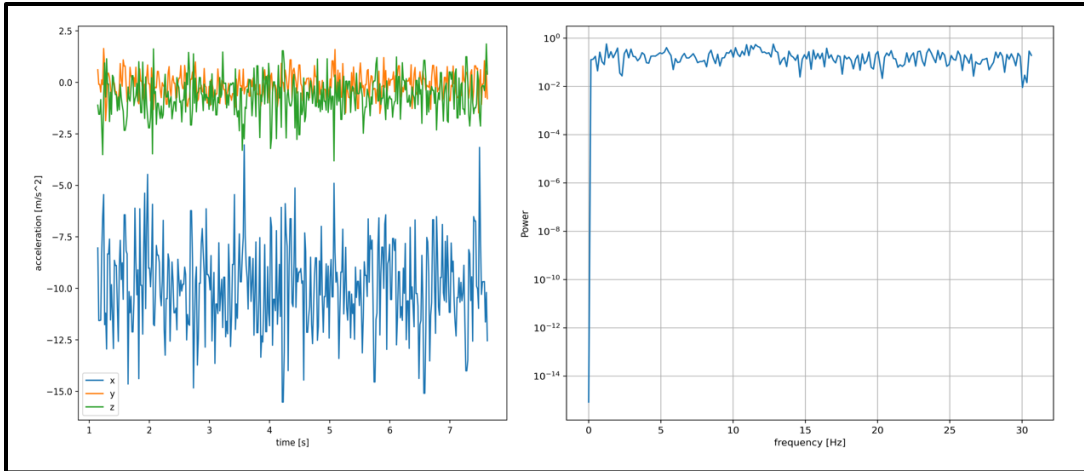


Figure 28. Sensor mount linear acceleration raw measurements (left). Acceleration frequency response (right)

To address the sensor mean displacement requirement, numerical integration to calculate mean sensor displacement over time would significantly propagate error, due to the very noisy and unreliable data collected (Cruz-Uribe, 2002). As shown in Figure 29, numerical integration yields a mean displacement of approximately 10 meters, which was certainly not the case.

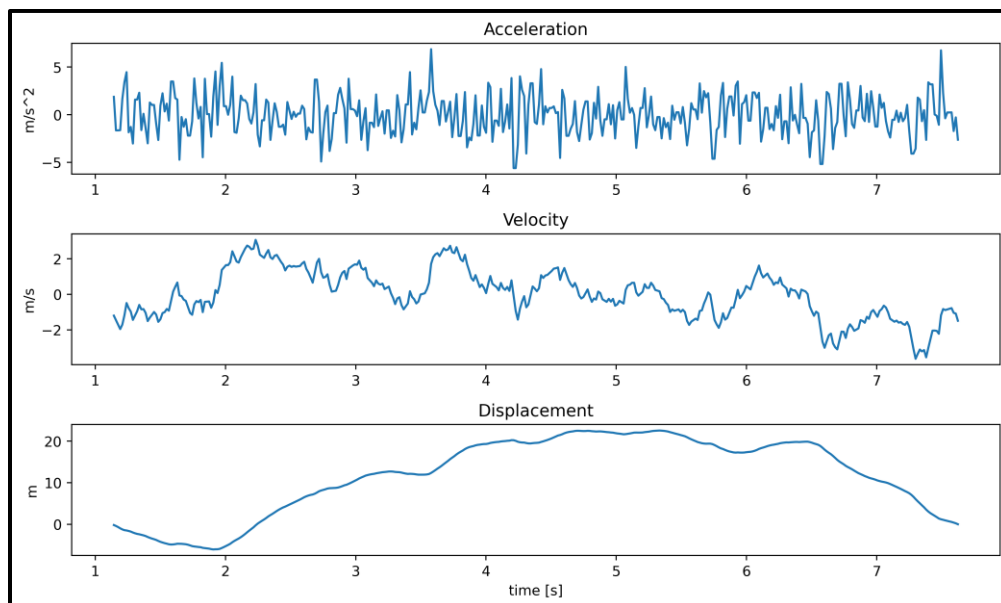


Figure 29. Displacement numerical integration results

As a result, the team looked at the dynamic response of the system to estimate the damping ratio of the sensor mount configuration. With a short-term Fourier transform, the team extracted time-dependent dominant frequencies, which were around 10 Hz as shown in Figure 30.

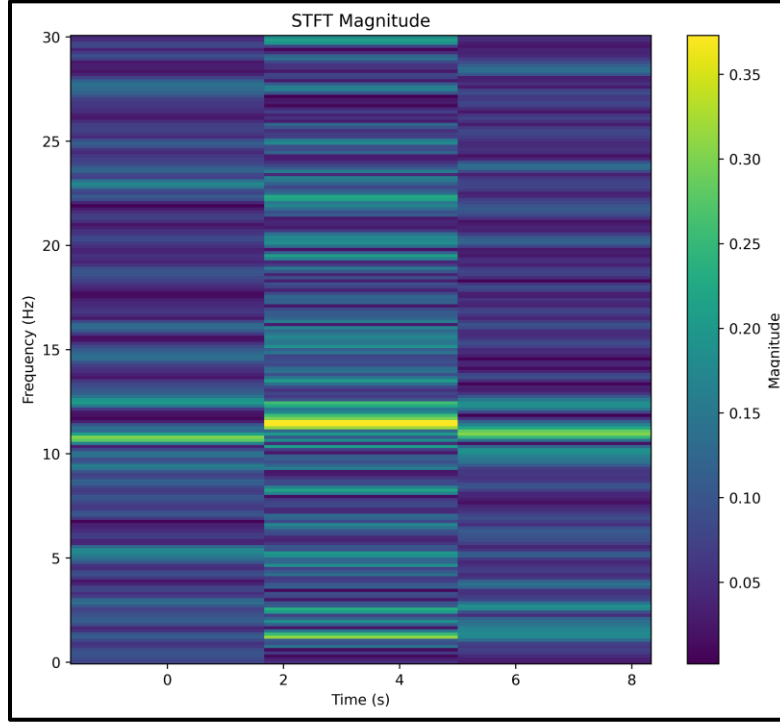


Figure 30. Short-term Fourier transform analysis to analyze time-dependent frequencies.

The damping ratio, ζ , can be approximated as a function of natural frequency and settling time (Ogata, 2010).

$$\zeta = \frac{4}{t_s \omega_n}$$

The settling time for this problem can be thought of how long the sensor mount in its vibratory state comes to rest after the robot wheels stop moving. The IMU measures roughly back to rest after $t_s = 0.033$ seconds. As a result for 10 Hz, the team's sensor configuration yields $\zeta = 1.93$, which satisfies the overdamped requirement ($\zeta > 1$) for

the team's sensor mount design. The team would like to emphasize that this analysis is not the main focus of the project but establishes a foundation for further research into the dynamics of the robot prototype.

8 ECONOMIC ANALYSIS

A rigorous evaluation of the final design also includes analyzing it at an economic level. By understanding the material and manufacturing costs associated with the development of the final system, the sponsor can make more informed decisions pertaining to its adoption and streamlining, i.e an economic analysis also provides more insights into more cost-efficient embedded system architectures and material selection.

To create an exhaustive economic analysis inclusive of time as a relevant cost for Tailos' efforts, once the bill of materials was finalized, all labor hours were tallied as the project constraints emphasize a strict manufacturing cost to be adhered to. The relevant labor hours include the time taken to post-process all 3D parts, assemble all components using needed fasteners, affix all sensors to the platform, wire, solder, and crimp the circuitry needed for the embedded system, and create a configuration. One should note that the time taken to develop all software, design all components, and time taken to print were not counted as labor hours as 3D prints are system performance dependent and all 'intellectual' based developments only occur once rather than repeatedly. Table 3 provides a summary of all associated costs incurred.

Table 3. Economic analysis with Labor, OEM & 3D parts as key factors

| Category | Parts/Time | Cost |
|-----------|--|----------|
| 3D Prints | Rear Panels, Front Panels, Optical Breadboard, Lidar Mount, Universal Mount, Jetson Enclosure | \$36.77 |
| OEM Parts | DSI Display Adapter, Camera Cable, M3 20mm Socket Head, M2 & M3 Heat-Set Insert, USB Hub, M4 <u>Torx</u> Countersink, M2-M4 Fastener Assortments, PLA Black Filament, PWM Servo Driver, Magnets. ICM-20948 9-axis IMU, Arduino Uno R3. | \$251.98 |
| Labor | \$35/ <u>hr</u> x (9 hours of circuitry work + 4.5 hours of post processing and assembly + 0.5 hour of configuration) | \$525 |

All 3D parts were printed with Ideamaker, an open-source 3D Slicing software. Ideamker provided a cost/mass estimate of 0.023\$/g; the total masses thus approximate to \$36.77. Compared to a 3D printing service such as Xometry, which provided a quote of \$368.54, it is apparent that directly printing the parts saves on shipping costs and time, which is in the interests of the sponsor to make rapid developments and adjustments as necessary. In terms of OEM parts other than the provided sensors, they were mostly comprised of breakout boards, circuit components, and fasteners with a combined cost of \$251.98. The OEM part costs when added to the 3D printed costs, provide a manufacturing cost of \$288.75, which is less than the budgetary constraint of \$300 established for the manufacturing cost. Overall, it is likely that with more careful circuitry topology and the use of PCBs, wiring costs can be cut significantly. Moreover, vibration tests were carried out with an Arduino Uno R3 logging IMU data as opposed to the onboard Jetson sampling directly. By utilizing the Jetson directly, costs can be further reduced.

Finally, in terms of labor costs, by using a mechanical engineering starting salary estimate of \$35 per hour, reflecting at a minimum the nature of the users who will be using

the platform, it was calculated that the combined total labor costs of \$525. However, with detailed documentations and revisions, this value can also be reduced.

Overall, it seems much of the costs were OEM component and assembly centric. An overhaul of the circuitry can significantly reduce the final costs associated with the design solution, even if it adheres to the constraints as is.

9 CONCLUSION & RECOMMENDATIONS

Overall, the final solution generally satisfies all requirements and constraints provided by the sponsor. Over time, the design solution evolved to emphasize conforming to the aesthetics of the existing PD1 chassis rather than solely emphasizing adjustability. As such, this resulted in a final design that conformed to the geometric constraints imposed by the robot's footprint. By using idea generation, morphological matrices paired with topology optimization, the final mechanical design was able to conform to the specifications without needing overhaul or repeated iterations. In terms of software and sensor coverage, the sensor placements qualitatively capture all needed FOVs but require a rigorous analysis by using RViz paired with the position/orientations via URDF.

In terms of recommendations pertaining to the functionality of the system in its ability to configure sensor suites, written software can further leverage URDFs and RViz to simulate sensor suites by enabling a desired sensor position or angular displacement as an input parameter and outputting a simulated visualized FOV of all sensors. For further adjustability, it may be effective to have the sensor mounts electronically adjustable by using servos with position readings provided by encoders. It may be possible to have these

position readings directly update an Rviz simulation, vastly shortening the time to update a configuration. Overall, this project lays the foundation for rapid optimizations of sensor suites and by extension, system-wide functionality in terms of robot navigation and control.

REFERENCES

- Avallone, E. A., Baumeister T., Sadegh A. (2006). *Marks' Standard Handbook for Mechanical Engineers*. McGraw-Hill Professional.
- Bhooshan, Shajay (2017, June 30). *Parametric design thinking: A case-study of practice-embedded architectural research*, Volume 52 pg. 115-143. *ScienceDirect*.
<https://doi.org/10.1016/j.destud.2017.05.003>
- Cruz-Uribe, D.; Neugebauer, C. J. (2002), "Sharp Error Bounds for the Trapezoidal Rule and Simpson's Rule" (PDF), *Journal of Inequalities in Pure and Applied Mathematics*, 3 (4)
- Farmiga, N. O., Jain, K. (1998). Three-dimensional universal mounting component system for optical breadboards (U.S. Patent No. 5,825,558). U.S. Patent and Trademark Office. <https://www.freepatentsonline.com/5825558.html>.
- Hendriks, B., et al. (2010). Robot vacuum cleaner personality and behavior. *International Journal of Social Robotics*, 3(2), 187-195. <https://doi.org/10.1007/s12369-010-0084-5>.
- Hershberger, D., Gossow, D., Faust, J., & Woodall, W. (2018, May 16). *Rviz*. ros.org. <https://wiki.ros.org/rviz>
- Kalis, R. M., Waite, S. P., et al. (2007). Separable ball and socket assembly for electronic device mounts (U.S. Patent No. 7,296,771). U.S. Patent and Trademark Office. <https://www.freepatentsonline.com/7296771.html>.
- Kristiawan, R. B., Imaduddin, F., Ariawan, D., Ubaidillah, & Arifin, Z. (2021). A review on the fused deposition modeling (FDM) 3D printing: Filament processing, materials, and printing parameters. *Open Engineering*, 11(1), 639-649.
- Lee, B. I., Ko, Y. H., et al. (2017). Robot vacuum cleaner (U.S Patent No. 10,918,250). U.S. Patent and Trademark Office.
[https://patents.google.com/patent/US10918250B2/en?q=\(robot+vacuum\)&oq=robot+vacuum&page=1](https://patents.google.com/patent/US10918250B2/en?q=(robot+vacuum)&oq=robot+vacuum&page=1)
- Luxonis, "Oak-D Pro Datasheet", Dec. 2021 [Revised Mar. 2022].
- NVIDIA, "NVIDIA Jetson Orin Nano Series Module Data Sheet", Sept. 2022 [Revised Apr. 2023].
- Ogata K. (2010). *Modern control engineering* (5th ed.). Prentice Hall.

- Open Robotics. (2023). Ros 2 documentation. ROS 2 Documentation - ROS 2 Documentation: Humble documentation. <https://ocs.ros.org/en/humble/>
- Otto, K. and Wood, K. (2001) *Product Design Techniques in Reverse Engineering and 13 New Product Development*. Prentice Hall, Upper Saddle River.
- Palacin, J., et al. (2003). Building a mobile robot for a floor-cleaning operation in domestic environments. *Proceedings of the 20th IEEE Instrumentation Technology Conference (Cat. No.03CH37412)*.
<https://doi.org/10.1109/imtc.2003.1207979>.
- Porter, M. (2015, October 20). *Damping evaluation*. Porter McGuffie, Inc. <https://pm-engr.com/damping-evaluation-2/>
- Prayash, H. S. H., Shaharear, M. R., Islam, M. F., Islam, S., Hossain, N., & Datta, S. (2019, November). Designing and optimization of an autonomous vacuum floor cleaning robot. In *2019 IEEE International Conference on Robotics, Automation, Artificial-intelligence and Internet-of-Things (RAAICON)* (pp. 25-30). IEEE.
- Raeburn, A. (2022, November 28). What is Extreme Programming (XP)? [2022]. Asana. <https://asana.com/resources/extreme-programming-xp>
- Shuhua, Wang & Qiaoli, Xu & Fen, Li & Jinming, Dai & Jia, Husheng & Bingshe, Xu. (2014). Preparation and properties of cellulose-based carbon microsphere/poly(lactic acid) composites. *Journal of Composite Materials*. 48. 10.1177/0021998313485263.
- Sucan, I., & Kay, J. (2023, March 24). *urdf*. ros.org. <http://wiki.ros.org/urdf>
- Tailos. (2023, August 30). Robot vacuums for hotels and residential buildings. <https://tailos.com/>.
- Ulrich, I., Mondada, F., & Nicoud, J. D. (1997). Autonomous vacuum cleaner. *Robotics and autonomous systems*, 19(3-4), 233-245.
- Ulrich, Karl T., et al. (2020). *Product Design and Development*. McGraw-Hill Education.

APPENDIX A: DATA SHEETS

DATA SHEET

NVIDIA Jetson Orin Nano Series

Ampere GPU + ARM Cortex-A78AE CPU + LPDDR5

NVIDIA Jetson Orin Nano Modules:

- Jetson Orin Nano 8GB (ON 8GB) - Ampere GPU + ARM Cortex-A78AE CPU + 8GB LPDDR5
- Jetson Orin Nano 4GB (ON 4GB) - Ampere GPU + ARM Cortex-A78AE CPU + 4GB LPDDR5

References to ON and Jetson Orin Nano can be read as Jetson Orin Nano 8GB and Jetson Orin Nano 4GB except where explicitly noted.

AI Performance

Jetson Orin Nano 8GB: Up to 40 (Sparse) INT8 TOPs and 20 (Dense) INT8 TOPs

Jetson Orin Nano 4GB: Up to 20 (Sparse) INT8 TOPs and 10 (Dense) INT8 TOPs

Ampere GPU

Jetson Orin Nano 8GB: 1024 NVIDIA® CUDA® cores | 32 Tensor cores

Jetson Orin Nano 4GB: 512 NVIDIA® CUDA® cores | 16 Tensor cores

End-to-end lossless compression | Tile Caching | OpenGL® 4.6 | OpenGL ES 3.2 | Vulkan™ 1.1⁵ | CUDA 10

Maximum Operating Frequency: 625 MHz

ARM Cortex-A78AE CPU

Six-core (ON 8GB and ON 4GB) Cortex A78AE ARMv8.2 (64-bit) heterogeneous multi-processing (HMP) CPU architecture | 2x clusters (1x 4-core cluster + 128 KB L1 + 256KB L2 per core + 2MB L3) + 1x 2-core cluster (128 KB L1 + 256KB L2 per core + 2MB L3) | System Cache: 4 MB (shared across all clusters)

Audio

Dedicated programmable audio processor | ARM Cortex A9 with NEON | PDM in/out | Industry-standard High-Definition Audio (HDA) controller provides a multi-channel audio path to the HDMI® interface

Memory

ON 8GB: 8GB 128-bit LPDDR5 DRAM

ON 4GB: 4GB 64-bit LPDDR5 DRAM

Secure External Memory Access Using TrustZone® Technology | System MMU | Maximum Operating Frequency: 2133 MHz

Networking

10/100/1000 BASE-T Ethernet | Media Access Controller (MAC)

Imaging

Eight lanes MIPI CSI-2 | D-PHY 2.1 (20 Gbps)

Display Controller

1x4K30 DP 1.2 (+MST for 2x 1080p60), HDMI 1.4, eDP 1.4

*See the Display section for more details on additional compatibility to DP 1.4a and HDMI 2.1

Maximum Resolution (eDP/DP/HDMI): up to 3840x2160 at 30 Hz

Multi-Stream HD Video and JPEG

Video Decode:

- Standards supported: H.265 (HEVC), H.264, VP9, AV1
 - 1x4K60 (H.265)
 - 2x4K30 (H.265)
 - 5x1080p60 (H.265)
 - 11x1080p30 (H.265)

Video Encode:

- 1080p30 Supported via CPU Cores with Software

Peripheral Interfaces

xHCI host controller with integrated PHY (up to) 3x USB 3.2, 3x USB 2.0 | 3 x1 (or 1 x2 + 1 x1) + 1 x4 (GEN3) PCIe | 3x UART | 2x SPI | 4x I²C | 1x CAN | DMIC | DSPK | 2x I²S | 15x GPIOs

Storage

Supports External Storage (for example: NVMe)

Mechanical

Module Size: 69.6 mm x 45 mm | 260 pin SO-DIMM Connector

Operating Requirements

Temp. Range (T_j): -25°C – 90°C | Supported Power Input: 5V

Jetson Orin Nano 8GB Modes: 7W | 15W

Jetson Orin Nano 4GB Modes: 7W | 10W

Note: Refer to the Software Features section of the latest L4T Development Guide for a list of supported features; all features may not be available.

⁵ Product is based on a published Khronos Specification and is expected to pass the Khronos Conformance Process. Current conformance status can be found at www.khronos.org/conformance.

* See the future Jetson Orin Nano Thermal Design Guide for details.

Figure A.1. Image of the Jeston Orin Nano data sheet (NVIDIA, 2022).

Table A.1. The different sensors and use cases (Tailos, 2023).

| Sensor | Proposed Use case |
|--|---|
| Luxonis Oak-D W Pro / rae | A direct replacement for the realsense camera. Provides up to 4 TOPS of processing power, which would allow us to run computer vision models on-device and save compute on the GPU. We would like to test CV models for the following tasks - (1) Detecting and picking debris (2) Cliff detection |
| Orbec Femto | A ToF based camera to provide a baseline comparison for depth sensing compared to the stereo vision based realsense. ToF cameras do not require contrast or feature rich surfaces and are less sensitive to environmental lighting conditions, and can potentially give us better results for cliff detection in brightly lit areas. |
| Arducam Multi-camera rig | Use multiple standalone RGB cameras connected to the Jetson platform to directly obtain the depth using monocular depth estimation from computer vision models. |
| Livox Mid-360 Lidar | Cost effective 3D lidar which will provide high accuracy point cloud data. Will increase accuracy of cliff detection and also help improve performance in dynamic environments. |
| Invensense Ultrasonic Sensor CH101-02ABR | ToF Ultrasonic sensors which can be used for both cliff detection and floor type detection. |

Ultra-Strength Lightweight Carbon Fiber Tube

Unidirectional Weave, 0.055" Wall Thickness, 0.610" OD, 6' Long

\$79.77 Each
5287T619



| | |
|------------------------------------|----------------------|
| Material | Carbon Fiber |
| Weave Type | Unidirectional |
| Appearance | Glossy, Plain |
| Shape | Round Tube |
| Texture | Smooth |
| Color | Black |
| Clarity | Opaque |
| Wall Thickness | 0.055" |
| Tolerance Rating | Standard |
| OD | 0.61" |
| OD Tolerance | -0.008" to 0.008" |
| ID | 1/2" |
| ID Tolerance | -0.003" to 0.003" |
| Wall Thickness Tolerance | -0.005" to 0.005" |
| Length | 72" |
| Length Tolerance | -0.03" to 0.03" |
| Hardness | Not Rated |
| Hardness Rating | Not Rated |
| For Use Outdoors | No |
| Temperature Range | -65° F to 180° F |
| Impact Strength | Not Rated |
| Impact Strength Rating | Not Rated |
| Tensile Strength | 125,000-175,000 psi |
| Tensile Strength Rating | Excellent |
| Straightness Tolerance | Not Rated |
| Compressive Strength | Not Rated |
| Flexural Strength | 100,000-150,000 psi |
| Flexibility | Rigid |
| Fiber Tensile Stiffness | Standard (33-36 msi) |
| Composite Tensile Stiffness | 14.8 msi |
| Composite Tensile Stiffness Rating | Good |
| Construction | Bidirectional |
| Construction Layup | 0°/90° |
| Density | 0.056 lbs./cu. in. |
| Dielectric Strength | Not Rated |

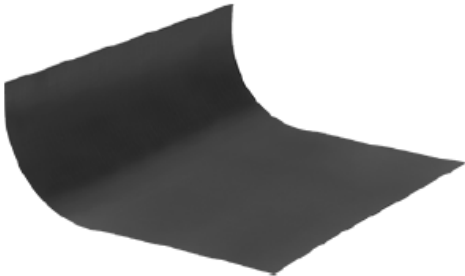

Figure A.2. Image of the carbon fiber tube data sheet (McMaster, 2023).



Flexible Magnet

with 1 Face, 1/32" Thick, 12" Wide, 24" Long

\$13.36 per pack of 1
5775K88

Holding Power on One Face

| | |
|------------------------------------|---|
| Shape | Rectangle |
| Mount Type | Standard |
| Thickness | 1/32" |
| Thickness Tolerance | -0.005" to 0.005" |
| Width | 12" |
| Width Tolerance | -0.36" to 0.36" |
| Length | 24" |
| Length Tolerance | -0.48" to 0.48" |
| Maximum Pull | 170 lbs. |
| Number of Faces with Holding Power | 1 |
| Sets of Poles | 14 poles per inch |
| Min. Temperature | 0° F |
| Maximum Temperature | 150° F |
| Material | Ceramic (Ferrite) |
| Color | Dark Brown |
| Maximum Energy Product | 5.6 kJ/m³ |
| Flux Density | 1,650 G |
| Fabrication | Bonded |
| Bonded With | Rubber |
| System of Measurement | Inch |
| RoHS | RoHS 3 (2015/863/EU) Compliant |
| REACH | REACH (EC 1907/2006) (06/14/2023, 235 SVHC) Compliant |
| DFARS | Specialty Metals COTS-Exempt |
| Country of Origin | United States |
| USMCA Qualifying | No |
| Schedule B | 850519.0000 |
| ECCN | EAR99 |

Figure A.3. Image of the magnet strip data sheet (McMaster, 2023).



Part No. 40-4040-Lite

40mm X 40mm Lite T-Slotted Profile - Four Open T-Slots

40-4040-Lite is a 40mm x 40mm lite metric 40 series square T-slot profile with four open T-slots, one on each 40mm face. The profile is smooth, which makes it resistant to dirt and debris buildup while also being easy to clean. The 40-4040-Lite profile is compatible with all 40 series fasteners. This profile lends itself to machine guards, enclosures, work benches, or displays. The four open T-slots enable access from any direction and are useful for mounting accessories.

Price Per Millimeter.....**\$0.0282**

*surcharge of \$2.79 per cut





Figure A.4. Image of the aluminum extrusion data sheet (80/20, 2023).

APPENDIX B: MORPHOLOGICAL MATRICES

Table B.1. Optical table with rectangular outer frame.

| Subfunction | Solutions | | | |
|---------------------|----------------------|-------------------|----------------------|--------------------|
| Stabilize Sensors | Optical Table | Magnets | Carbon Fiber Tubes | Aluminum Extrusion |
| Position Sensors | Rectangular Platform | Cylindrical Beams | Ball & Socket Joints | Rectangular Beams |
| Secure Jetson | Middle of Robot | Back of Robot | | |
| Divide Sensor Ports | DIN Rail | Direct Mounting | | |

Table B.2. Aluminum extrusion with rectangular outer frame design.

| Subfunction | Solutions | | | |
|---------------------|----------------------|-------------------|----------------------|--------------------|
| Stabilize Sensors | Optical Table | Magnets | Carbon Fiber Tubes | Aluminum Extrusion |
| Position Sensors | Rectangular Platform | Cylindrical Beams | Ball & Socket Joints | Rectangular Beams |
| Secure Jetson | Middle of Robot | Back of Robot | | |
| Divide Sensor Ports | DIN Rail | Direct Mounting | | |

Table B.3. Magnets with arm & socket joints design.

| Subfunction | Solutions | | | |
|---------------------|----------------------|-------------------|----------------------|--------------------|
| Stabilize Sensors | Optical Table | Magnets | Carbon Fiber Tubes | Aluminum Extrusion |
| Position Sensors | Rectangular Platform | Cylindrical Beams | Ball & Socket Joints | Rectangular Beams |
| Secure Jetson | Middle of Robot | Back of Robot | | |
| Divide Sensor Ports | DIN Rail | Direct Mounting | | |

Table B.4. Carbon fiber tubes with cylindrical outer frame design.

| Subfunction | Solutions | | | |
|---------------------|----------------------|-------------------|----------------------|--------------------|
| Stabilize Sensors | Optical Table | Magnets | Carbon Fiber Tubes | Aluminum Extrusion |
| Position Sensors | Rectangular Platform | Cylindrical Beams | Ball & Socket Joints | Rectangular Beams |
| Secure Jetson | Middle of Robot | Back of Robot | | |
| Divide Sensor Ports | DIN Rail | Direct Mounting | | |

APPENDIX C: BACK OF ENVELOPE CALCULATIONS (BOE)

optical Table

$$W = 250 \text{ mm} = 25 \text{ cm}$$
$$L = 515 \text{ mm} = 51.5$$
$$h = 4 \text{ mm} = 0.4 \text{ cm}$$
$$\rho = 1.23 \text{ g/cm}^3$$
$$m = \rho L W h = \frac{1.23 \text{ g}}{\text{cm}^3} (25 \cdot 51.5 \cdot 0.4)$$
$$= 633.45 \text{ g}$$

Spool of PETG = \$20

$$\frac{\$20}{1000 \text{ g}} = \$0.02/\text{g}$$
$$\text{Cost} = 0.02 (633.45) = \$12.67$$

Figure C.1. BOE calculations for mass and cost of the optical table design.

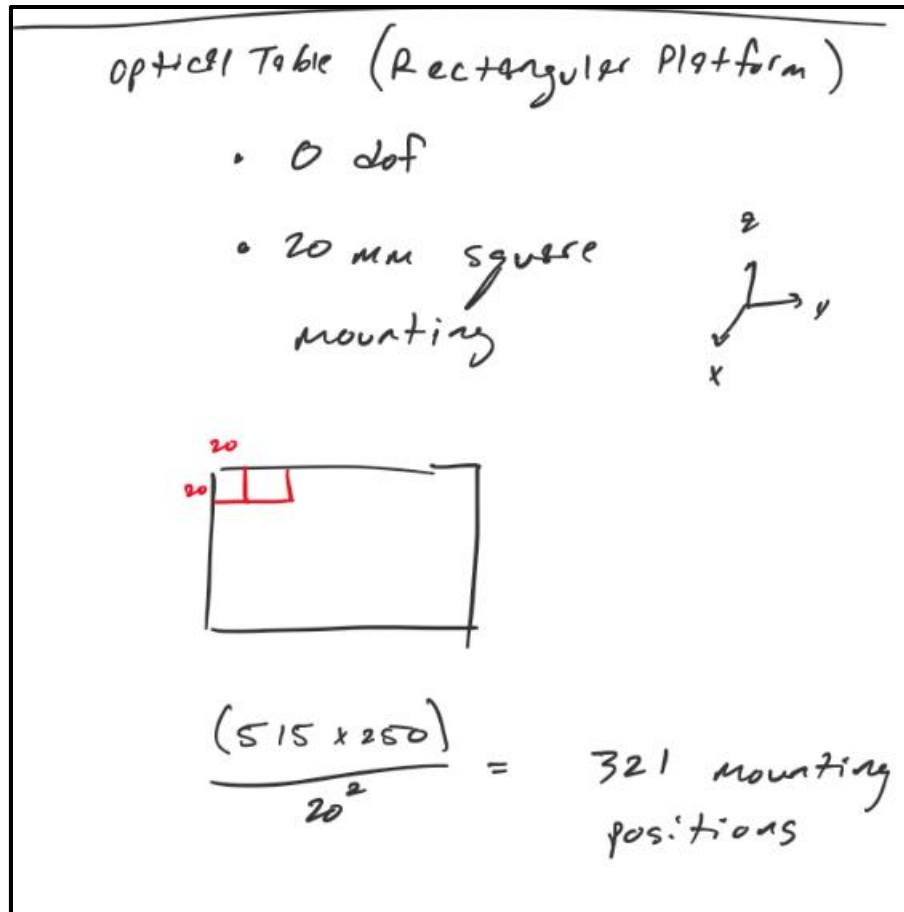


Figure C.2. BOE calculations for degrees of freedom (DOF) and mounting positions of the rectangular platform.

Aluminum Extrusion

$$L = 515 \text{ mm}$$

$$W = 250 \text{ mm}$$

$$\bar{\lambda}_m = \frac{m}{L} = 0.0016 \frac{\text{kg}}{\text{mm}}$$

$$\bar{\lambda}_\$ = \frac{\$}{L} = 0.0256 \$/\text{mm}$$

$$m = (2L\bar{\lambda}_m + 2W\bar{\lambda}_m) \cdot 1000$$

$$= (2 \cdot 515 \cdot 0.0016 + 2 \cdot 250 \cdot 0.0016) 1000$$

$$= 2371.61 \text{ g}$$

$$\text{cost} = (2L\bar{\lambda}_\$ + 2W\bar{\lambda}_\$)$$

$$= \$39.17$$

Figure C.3. BOE calculations for mass and cost of the aluminum extrusion design.

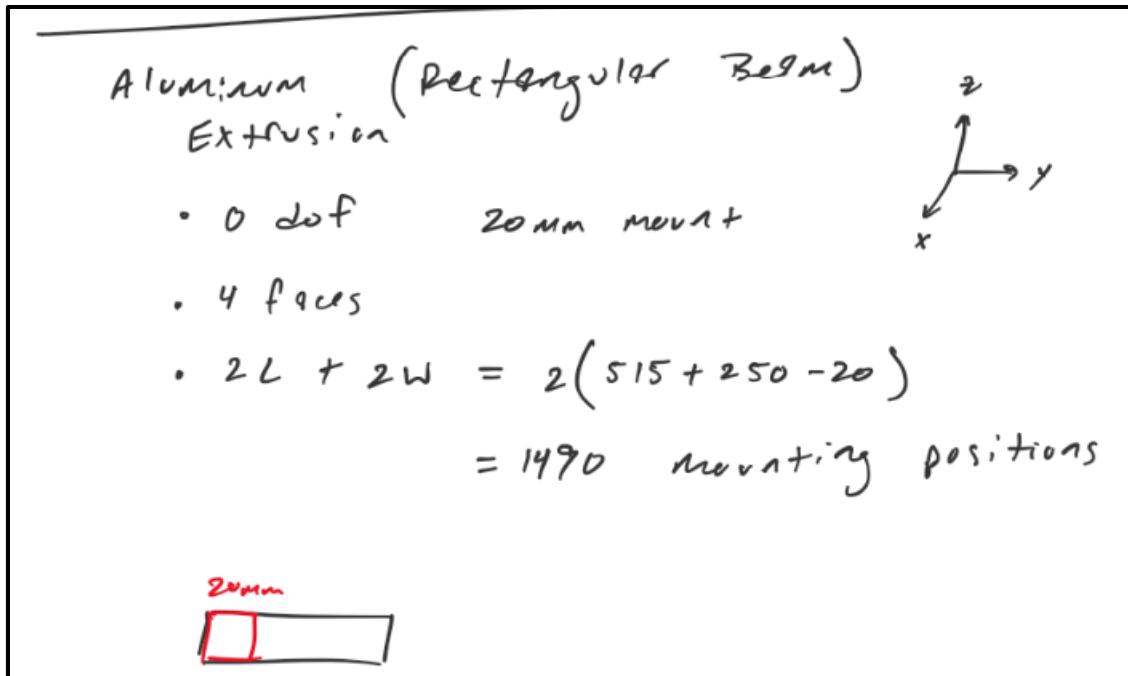


Figure C.4. BOE calculations for DOF and mounting positions of the rectangular beams.

Carbon Fiber Tube

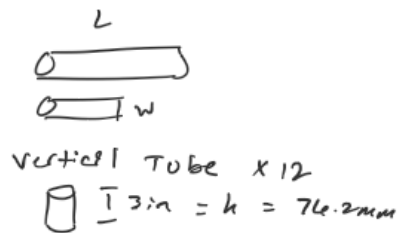
$$D = 15.5 \text{ mm}$$

$$d = 12.7 \text{ mm}$$

$$\rho = 1.56 \times 10^{-6} \frac{\text{kg}}{\text{mm}^3}$$

$$L = 515 \text{ mm}$$

$$W = 250 \text{ mm}$$



$$V = 2\pi \left[\frac{(D-d)}{2} \right]^2 L + 2\pi \left[\frac{(D-d)}{2} \right]^2 W + 12\pi \left[\frac{(D-d)}{2} \right]^2 h$$

$$V = 24,367.68 \text{ mm}^3$$

$$m = \rho V = 1.56 \times 10^{-6} (24,367.68)$$

$$= 37.77 \text{ g}$$

$$\bar{A}_f = 0.0436 \text{ g/mm}$$

$$\text{Cost} = (2L \bar{A}_f + 2W \bar{A}_f) + 12h \bar{A}_f$$

$$= \$173.36$$

Figure C.5. BOE calculations for mass and cost of the carbon fiber tube design.

CF Tubes (Cylindrical Beam)

1 dof

$$4(515 + 250 - 20)$$


$$= 2980 \text{ mounting positions}$$


Figure C.6. BOE calculations for DOF and mounting positions of the cylindrical beams.

magnets

$$L = 515 \text{ mm}$$

$$W = 250 \text{ mm}$$

$$t = 0.79375 \text{ mm}$$

$$\rho = 4.982 \times 10^{-6} \text{ kg/mm}^3$$

$$m = (\rho L W t) 1000 = 509.13 \text{ g}$$

$$\$13.36 \text{ for } L = 24", W = 12", t = 1/32"$$

$$\$/\text{in}^3 = \frac{\$13.36}{(24 \cdot 12 \cdot 1/32)} = \$1.484/\text{in}^3$$

$$\frac{1.484 / \text{in}^3}{16387.1 \text{ mm}^3} = \$9.0586 \times 10^{-5} / \text{mm}^3$$

$$V = 102195.3125 \text{ mm}^3$$

$$\begin{aligned} \text{Cost} &= \$/\text{mm}^3 (V) \\ &= \$9.26 \end{aligned}$$

Figure C.7. BOE calculations for mass and cost of the magnets design.

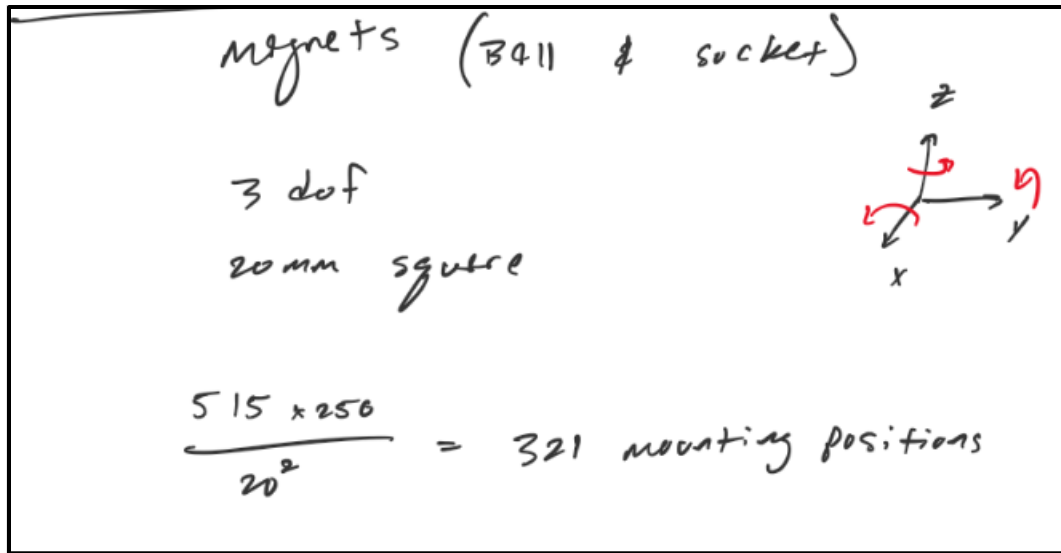


Figure C.8. BOE calculations for DOF and mounting positions of the ball & socket.

APPENDIX D: PUGH CHARTS

Table D.1. Pugh chart with the Optical Table design as the datum.

| Datum: Optical Table | Criteria | Optical Table | Aluminum Extrusion | Carbon Fiber Tubes | Magnets |
|----------------------|-------------------------|---------------|--------------------|--------------------|----------|
| | Weight | 0 | - | + | + |
| | # of DOF | 0 | 0 | + | + |
| | # of Mounting Positions | 0 | + | + | 0 |
| | Cost | 0 | - | - | + |
| | Customer Preference | 0 | 0 | - | - |
| | Ease of Access/Mounting | 0 | + | + | 0 |
| | Sum of + | 0 | 2 | 4 | 3 |
| | Sum of - | 0 | -2 | -2 | -1 |
| | Sum | 0 | 0 | 2 | 2 |

Table D.2. Pugh chart with the Aluminum Extrusion design as the datum.

| Datum: Aluminum Extrusion | Criteria | Optical Table | Aluminum Extrusion | Carbon Fiber Tubes | Magnets |
|---------------------------|-------------------------|---------------|--------------------|--------------------|----------|
| | Weight | + | 0 | + | + |
| | # of DOF | 0 | 0 | + | + |
| | # of Mounting Positions | - | 0 | + | - |
| | Cost | + | 0 | - | + |
| | Customer Preference | 0 | 0 | - | - |
| | Ease of Access/Mounting | - | 0 | 0 | - |
| | Sum of + | 2 | 0 | 3 | 3 |
| | Sum of - | -2 | 0 | -2 | -2 |
| | Sum | 0 | 0 | 1 | 1 |

Table D.3. Pugh chart with the Carbon Fiber Tubes design as the datum.

| Datum: Carbon Fiber Tubes | Criteria | Optical Table | Aluminum Extrusion | Carbon Fiber Tubes | Magnets |
|---------------------------|-------------------------|---------------|--------------------|--------------------|-----------|
| | Weight | - | - | 0 | - |
| | # of DOF | - | - | 0 | + |
| | # of Mounting Positions | - | - | 0 | - |
| | Cost | + | + | 0 | + |
| | Customer Preference | + | + | 0 | 0 |
| | Ease of Access/Mounting | - | 0 | 0 | - |
| | Sum of + | 2 | 2 | 0 | 2 |
| | Sum of - | -4 | -4 | 0 | -4 |
| | Sum | -2 | -2 | 0 | -2 |

Table D.4. Pugh chart with the Magnets design as the datum.

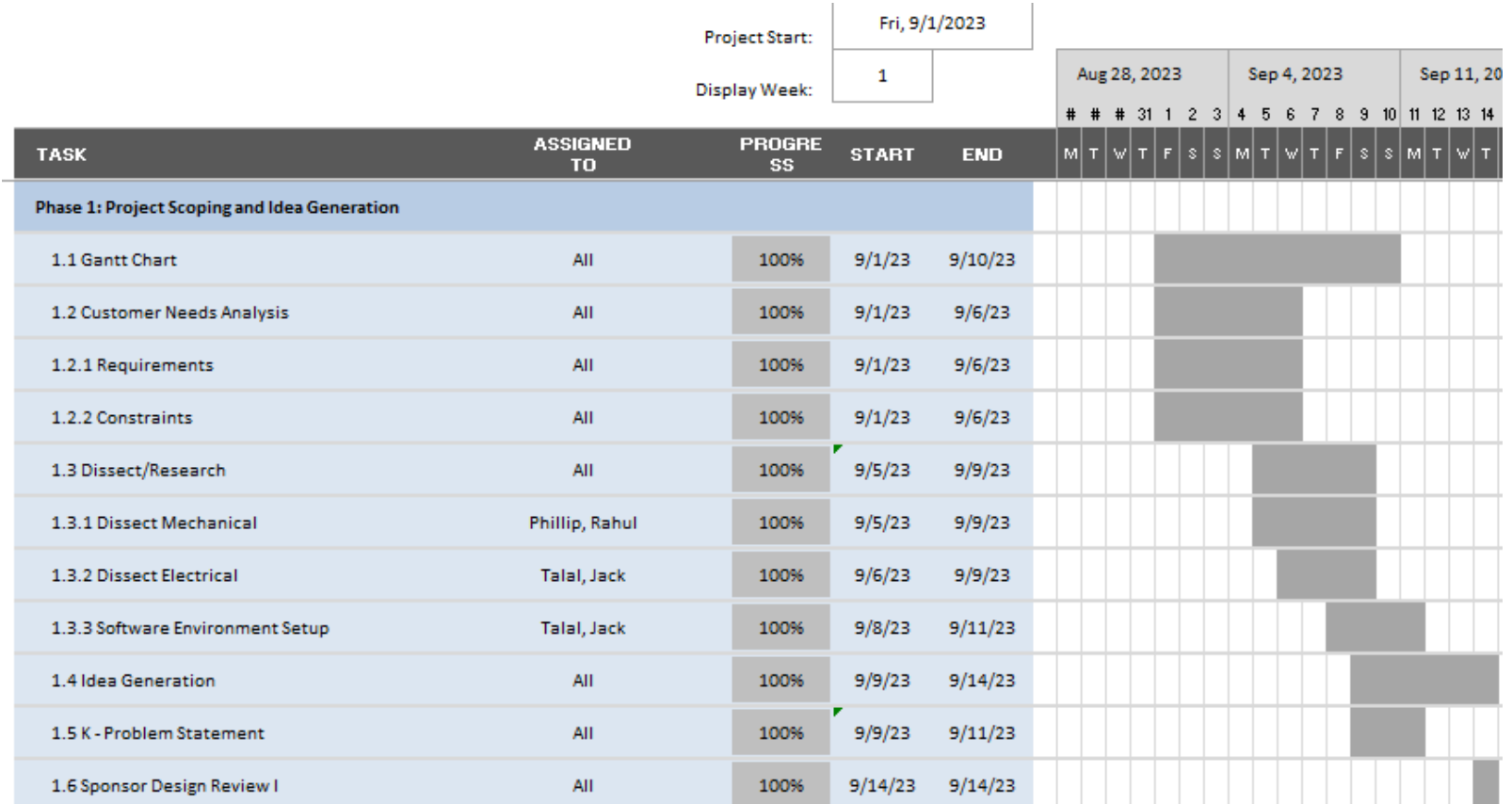
| Datum: Magnets | Criteria | Optical Table | Aluminum Extrusion | Carbon Fiber Tubes | Magnets |
|----------------|-------------------------|---------------|--------------------|--------------------|----------|
| | Weight | - | - | + | 0 |
| | # of DOF | - | - | - | 0 |
| | # of Mounting Positions | 0 | + | + | 0 |
| | Cost | - | - | - | 0 |
| | Customer Preference | + | + | 0 | 0 |
| | Ease of Access/Mounting | 0 | + | + | 0 |
| | Sum of + | 1 | 3 | 3 | 0 |
| | Sum of - | -3 | -3 | -2 | 0 |
| | Sum | -2 | 0 | 1 | 0 |

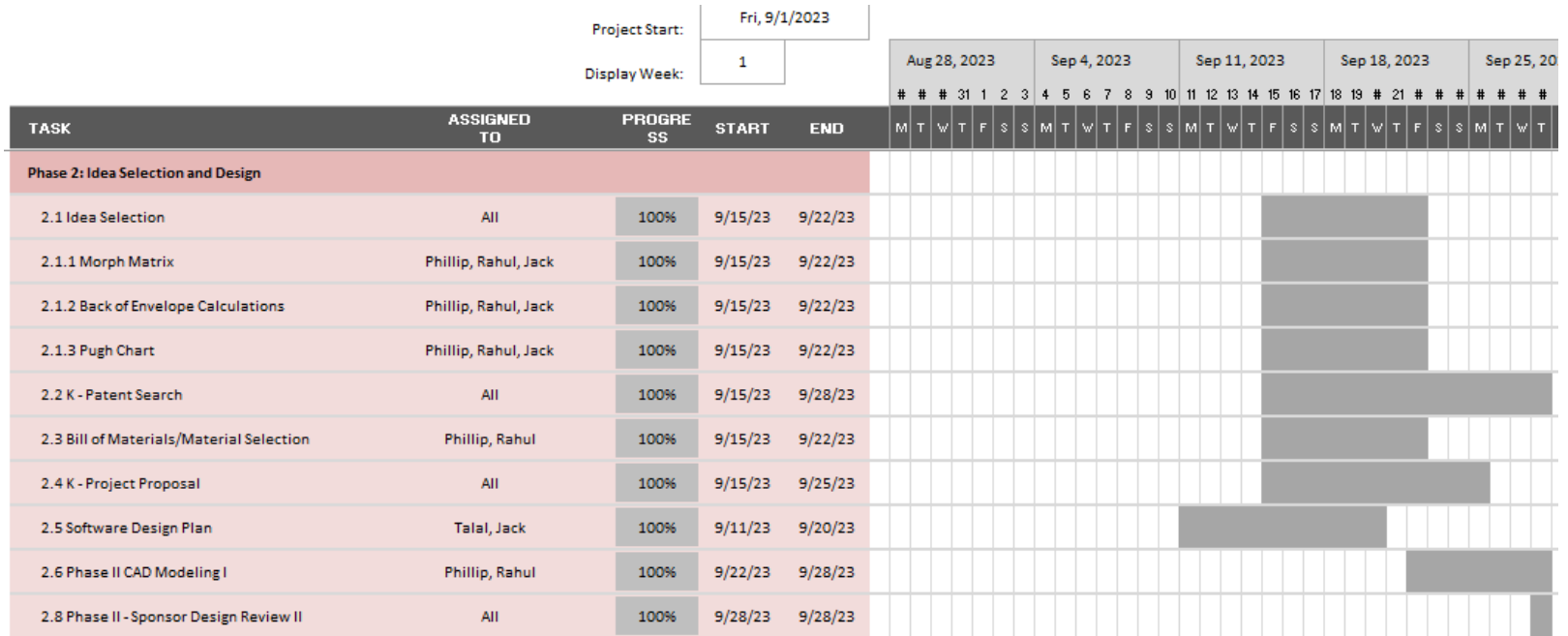
APPENDIX E: BILL OF MATERIALS

Table E.1. Bill of Materials table.

| Item | Manu # | Vendor | Description | Price | Qty | Total | Link |
|--------------|-----------|----------|---|---------|-----|-----------------|--|
| 1 | B094WC6 | Amazon | Compute Module DSI Display Adapter, 22PIN to 15PIN Adapter, for Official Compute Module 4 IO Board and Waveshare Compute Module IO Board, Comput | \$8.99 | 1 | \$8.99 | https://www |
| 2 | B092HDC | Amazon | MELIFE 3 Pcs 3.28FT for Raspberry Pi Camera Cable, Octoprint Octopi Webcam for Monitor 3D Printer, 100CM Long Extension Flex Ribbon Cable for RPi. | \$5.99 | 2 | \$11.98 | https://www |
| 3 | 91292A12 | McMaster | 18-8 Stainless Steel Socket Head Screw M3 x 0.5 mm Thread, 20 mm Long | \$8.18 | 1 | \$8.18 | https://www |
| 4 | 94459A42 | McMaster | Heat-Set Inserts for Plastic Aluminum, M3 x 0.5 mm, 5.9 mm Installed Length | \$7.55 | 1 | \$7.55 | https://www |
| 5 | 94459A41 | McMaster | Heat-Set Inserts for Plastic Aluminum, M2 x 0.4 mm, 4.1 mm Installed Length | \$7.75 | 1 | \$7.75 | https://www |
| 6 | USBG-BRE | USBgear | 4-Port USB 3.2 Gen 1 Mountable Charging and Data Hub | \$24.19 | 1 | \$24.19 | https://www |
| 7 | 95893A23 | McMaster | Flat Head Thread-Forming Screws for Plastic Torx Drive, 90 Degree Countersink, M4 Size, 10 mm Long | \$7.05 | 1 | \$7.05 | https://www |
| 8 | 95893A23 | McMaster | Flat Head Thread-Forming Screws for Plastic Torx Drive, 90 Degree Countersink, M4 Size, 12 mm Long | \$7.41 | 1 | \$7.41 | https://www |
| 9 | B089K35L | Amazon | VIGRUE 1230 Pieces M2 M3 M4 M5 Flat Head Socket Cap Screws 304 Stainless Steel Cap Bolts Nuts Washers Assortment Kit with 4Pcs Hex Wrenches | \$26.99 | 1 | \$26.99 | https://www |
| 10 | B0BKQ6T8 | Amazon | HELIFOUNER 1280 Pieces M2 M2.5 M3 M4 304 Stainless Steel Phillips Pan Head Machine Screws, Metric Screws Bolts Washers Nuts Kit, 304 Stainless Steel | \$19.99 | 1 | \$19.99 | https://www |
| 11 | BOC6T2PM | Amazon | Creality 3D Printer Filament, PLA Filament 1.75mm Bundle 2Kg for 3D Printing, Ender PLA Filament No-Tangling, Strong Bonding & Overhang Performance, | \$29.99 | 1 | \$29.99 | https://www |
| 12 | | | Rear Panel | \$4.84 | 2 | \$9.68 | |
| 13 | | | Front Panel | \$5.53 | 2 | \$11.06 | |
| 14 | | | Optical Breadboard | \$6.49 | 1 | \$6.49 | |
| 15 | | | Lidar Mount | \$1.32 | 1 | \$1.32 | |
| 16 | | | Universal Mount | \$1.32 | 2 | \$2.64 | |
| 17 | | | Jetson Enclosure | \$5.58 | 1 | \$5.58 | |
| 18 | 815 | Adafruit | Adafruit 16-Channel 12-bit PWM/Servo Driver - I2C interface - PCA9685 | \$14.95 | 1 | \$14.95 | https://www |
| 19 | B09Y82M1 | Amazon | MIKEDE Rare Earth Magnets with Hole, 50Pcs Strong Neodymium Disc Magnets with Stainless Screws for Wall Mounting, Small Roud Magnets with Counte | \$8.99 | 1 | \$8.99 | https://www |
| 20 | B01CJE0ZL | Amazon | Areyourshop 10 Pcs 5.5mm x 2.5mm CCTV Camera DC Power Male Jack Connectors | \$11.99 | 1 | \$11.99 | https://www |
| 21 | B01LH1FR | Amazon | Striveday Flexible Silicone Wire 22awg Electric Wire 22 Gauge Tinned Copper Hook Up Wire 300V Cables Electronic Stranded Wire Cable Electrics DIY Box-1 | \$14.99 | 1 | \$14.99 | https://www |
| Total | | | | | | \$247.76 | \$210.99 |

APPENDIX F: GANTT CHART





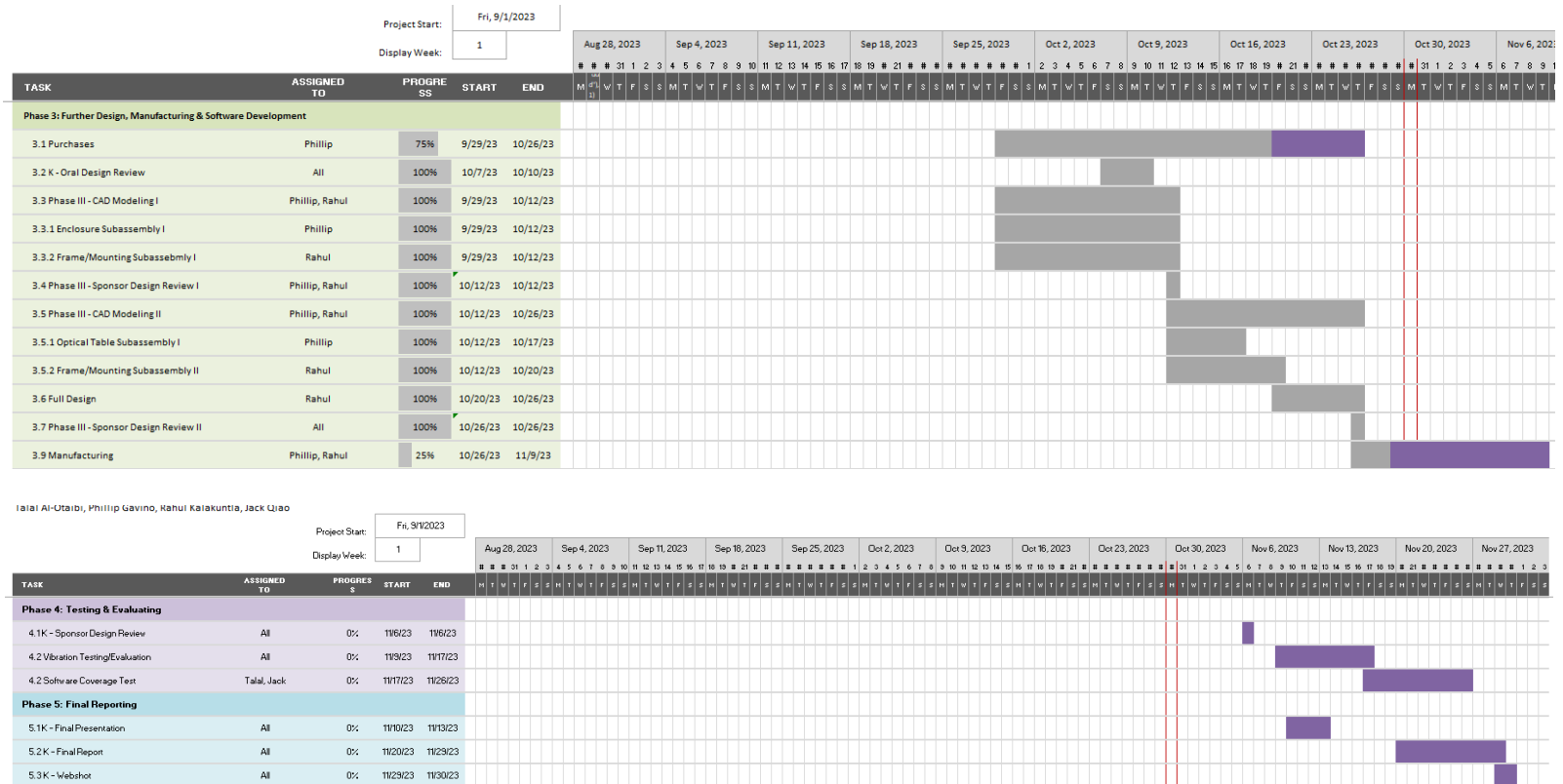


Figure F.1. Image of the Gantt chart.